Errera Rules !

Antoine Lizée

August 21, 2011

This is the internship report that summarizes the four month (April-July) spent by Antoine Lizée as an intern of the Dumais Laboratory, in the Department of Organismic and Evolutionary Biology of Harvard University.

Acknowledgments

I would like to thank for the wonderful four months I spent in the heart of Cambridge:

- David Quéré for his inspiring courses back on Palaiseau's plateau and his great help for finding this internship.
- Pr. Jacques Dumais, for his everyday support and enlightenment concerning the project.
- Jacques Dumais, Mariela and Marina for their incredibly warm welcome.
- Sebastien Besson, for his availability and pedagogy about the work he lead before me.
- Ben, Tony, and the French 'Plasmode' team for their everyday tips and friendship.

Less personal thoughts go toward two institutions that make my internship easier:

- The chair 'X Saint-Gobain' for their financial support.
- The developing team of Geogebra, which has developed an incredibly simple yet powerful geometrical tool for free, which helped me during my reflection.

Table of contents

Introduction

1. Plant cell division, rules and geometry

1.I. Errera's rule

Cell division in plant tissues is one of the - few? - Biological processes which do not make a physicist mad by its complexity or unpredictability. Indeed, since the end of the 19th century, two statements concerning cell division in plant tissues have proven out to be so well followed by nature that they have reached the golden state of 'laws':

- Sach's rule states that the division leads to two daughter cells with equal volume. REF
- Errera's rule (1888) states that the dividing wall takes the shape a soap film would take under the same conditions. You can observe the results of cross observations between real cell shapes and soap films in figure 1. REF

These two rules and especially Errera's rule characterize an optimization process which enables the cell to conserve time, material and energy. Indeed, its surface tension gives the soap film an optimal shape with regards to its area. The cell 'chooses' the plane of division that minimize its area under the constraint of volume. Although the molecular processes underneath this optimization is not yet well understood, these rules have been tested and approved to a large extend – despite several exceptions stored by botanists.

1.II. Geometry and Probability

This large verification of what I will name from now "Errera's rules" has been carried out mainly on 2D tissues whose third dimension is just an extrusion of the 2D pattern, like epidermal tissues. For these cell "tilings", every calculation can be done in the plane, and Errera's rules applied to 2D patterns lead to one beautiful geometric rule: the geometrical result of this optimization is that the dividing wall, in theory, must be an arc of circle with right angles at its connections with the existing walls of the mother cell. My worst misnomer will be to recall this particular shape for the dividing wall by "Errera shape".

There can be several planes of divisions that have this Errera shape. These planes are all local minima in terms of area, and if the volume ratio of division is V/2, then there is at most one dividing plane for each couple of edges of the mother cell. The strict optimization of the process would lead to the cell choosing the global minimum, i.e. the wall that has the lower area among the several planes with Errera shape satisfying this volume constraint. Recent observations developed in Dumais Laboratory REF has shed light on a probabilistic behavior, stating that the dividing wall will finally be chosen among the candidates with a probability relying on the difference in area between this final wall and the global minimum. This dependence seems to be exponential.

2. My work in the Dumais Laboratory

I arrived in the Dumais Laboratory just after the publishing of the paper that shed light on the elegant probabilistic observation cited above. My work was to explore new way of analyzing and comparing these rules with real phenomenon. As a matter of fact, and because all started with MATLAB, I have worked mostly with this powerful tool I needed first to master – I have very little formation in computing and had never worked with MATLAB before. Sebastien Besson, a (French) postdoc who had worked a lot on this project before me, have spent several years building a set of MATLAB function and programs to numerize, create, compute, merge, divide and more broadly to study plant tissues. I have created other Matlab programs in this environment, in order to broaden this study of cell tissues and to carry on new simulations. My work can be organized in two parts:

1. The creation of tools to study more deeply division of plant cell on flat tissues through the simulation of tilings. To achieve this goal, I have created a tool of quantitative comparison between different tilings, to compare simulation and reality more accurately than usual observations. Additionally, my main achievement is the creation of a program that computes analytically the different results of Errera's division.

2. The research of solutions that would be the product of Errera's division on a cone. This is another way to explore Errera's rules of division, with a different approach. Indeed, the tissues at work are conic rather than flat and thereby can describe more precisely meristems, which is a crucial system for cell division in plants.

This report is mainly meant to be the key of understanding of the work I have done in the lab, especially as this work is to be continued. Provided the computational and geometrical core of what I present, this report could therefore become a little heavy in details and explanations. Forewarned is forearmed…

Part I:
Simulation of tilings

1. Quantitative comparison of tissues

1.I. Topologic tool

Comparing tissues is like comparing faces, it first relies on one's feeling. But when it is very difficult to make an objective comparison, the pattern nature of tissues facilitates the findings of objective criteria that could be used to compare them. The main criterion that is used in the current literature is the topological one. The distribution of the number of edges for each cell is a really convenient measure, and is for sure an objective criterion to compare cell tilings, but it characterizes only partially the tissue. Although many hasty conclusions can be found in the literature, this topological comparison seems not sufficient to tell if tilings are similar, and to draw precise conclusion about the relevance of a simulation for instance. Thus, I have tried to develop a new tool for comparing tissues based on the statistical description of the geometry of the tiling.

1.II. A new tool

1.II.a Introduction

I have designed a tool that enables to compare tissues from another point of view. We want to estimate and quantify the regularity of the tissue, and we need a convenient representation or values that translate the information we have extracted. If we want to go from scratch, there is actually many degrees of freedom used to define the shape of one cell. More exactly, since we are working on 2D tissues, the counting of the coordinates of the non-fixed vertices leads to: $N_{DOF} = 2(n-1)$, n being the number of edges of the cell. Theses coordinates are not convenient parameters to describe the geometry of the cell, but above all they are far too numerous to lead to a clear representation of the shape of the cell or the geometry of the tissue. Instead of looking for a complex function that would give a few variables to characterize the cell from all these freedom degrees, I have chosen to change the scale of description of the tissue and to characterize the tissue from its vertices. Indeed, the roles of the vertices in the cell are quite symmetric, all the more as we are describing tissues in their whole and not a few cells.

1.II.b Edge plotting

We try to make a visual characterization of these vertices by plotting each vertex with the three edges on a polar plot. Actually, we represent only the extremities of the edges, and we stack all the vertices. Then, we have to treat and sort these edges in relation to the degrees of freedom left: the three angles that separate the edges and their lengths.

To enhance the visualization of the data, we have decided to sort the three edges of each vertex by putting one particular edge on the right abscissa axis. The most meaningful choice has proven out to be the edge in front of the biggest of the three angles, which is very often the younger edge. Since we don't want to keep any information on the absolute orientation of these vertices, we also flip each vertex if needed in order to put the biggest angle of the two remaining on the top of the graph, as shown in Figure 1.

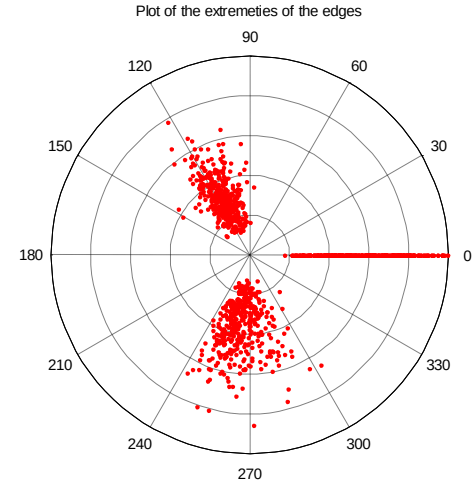

Figure 1. Polar plot of edge sorting.

1.II.c Statistical data

This characterization is a new and potentially powerful mean to compare tissues. We still need to describe more accurately the features of the tissue as a whole, thus to use a statistical description of our edge plotting. We will characterize, after sorting, the angles and length by classic statistical values and functions: mean, standard deviation, and histograms. This gives us the real means to compare tissues. We do not deal directly with the quite messy representation of our edge plotting. The program gives finally a clear output depending on the different options that you can enter as inputs, and below is a classic example of the statistical data we get to finally compare characterize and compare tissues from a geometrical point of view.

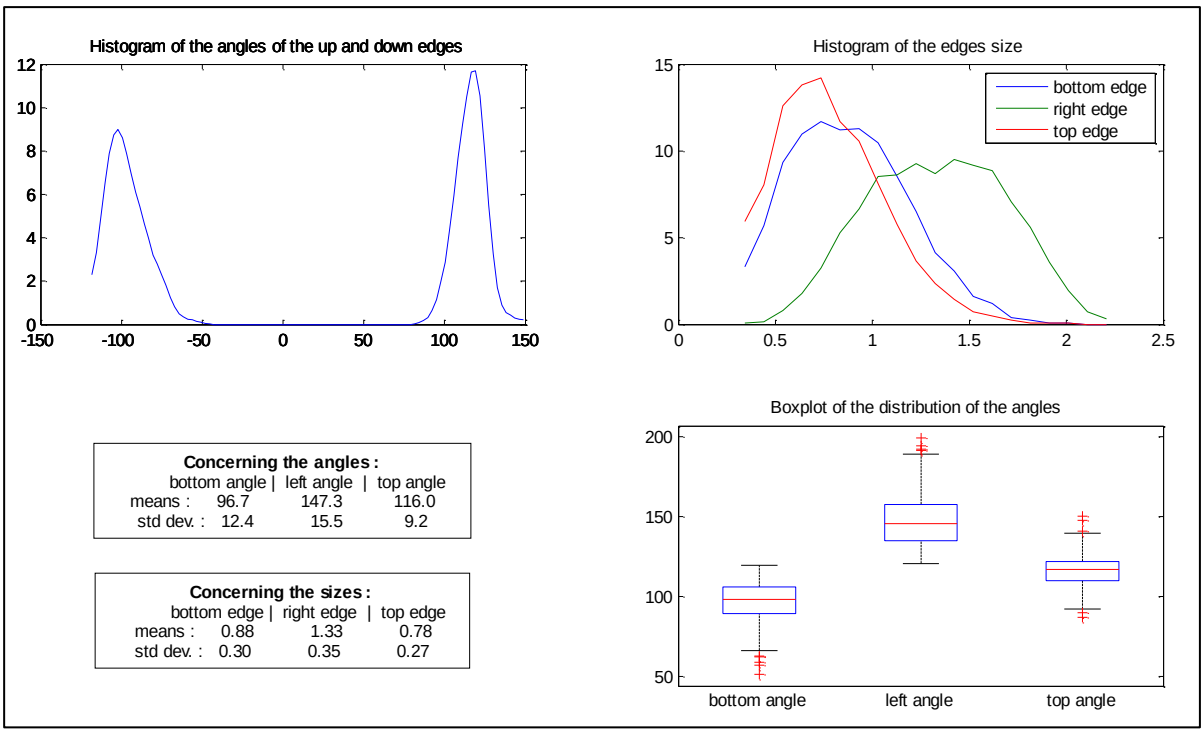

Figure 2. Output of the plotedges function to quantitatively study tissue geometry.

From upper left to bottom right: repartition of edges in relation to the angular values of the two smallest angles of the three; repartition of edges in relation to their size for the three types of edges per vertex; main statistical values; boxplot of the three angles.

1.III. Tests and Conclusions

If we consider the results given by our program, we can carry out a proof of principle of our approach from tissues whose origin we know. We have compared 6 tissues, 5 of them being observed from the same system of the species “Microsorum”, and the last, about four times bigger, is of a close species of fern, “Zinnia”. The complete study of the tool through these tests is, again, attached to this document as an annex. The conclusions are positive. The topological study could not give us clear or even precise results (see Figure 4): it is quite hard to group the characteristics of the Microsorum tissues, and to differentiate it from the topological characterization of the Zinnia tissue. Even though it exists a real difference between the topology of the Microsorum tissues taken as one and the Zinnia tissue, this difference is not clear and does not provide any information about how these tissues are different.

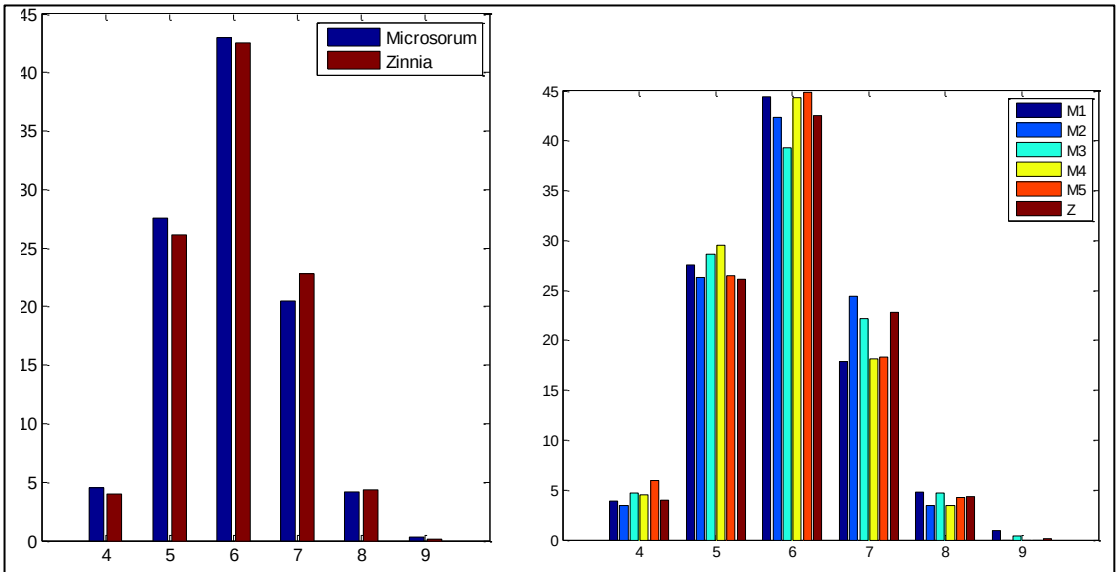

Figure 4. Topological characterization of the test tissues

However, our 'plotedge' technique can go a step further, as shown in the precise study in annex. I have reproduced a figure of this annex below, to underline how precisely this process take advantage of intrinsic features of the tissues (here, the difference of division activity).

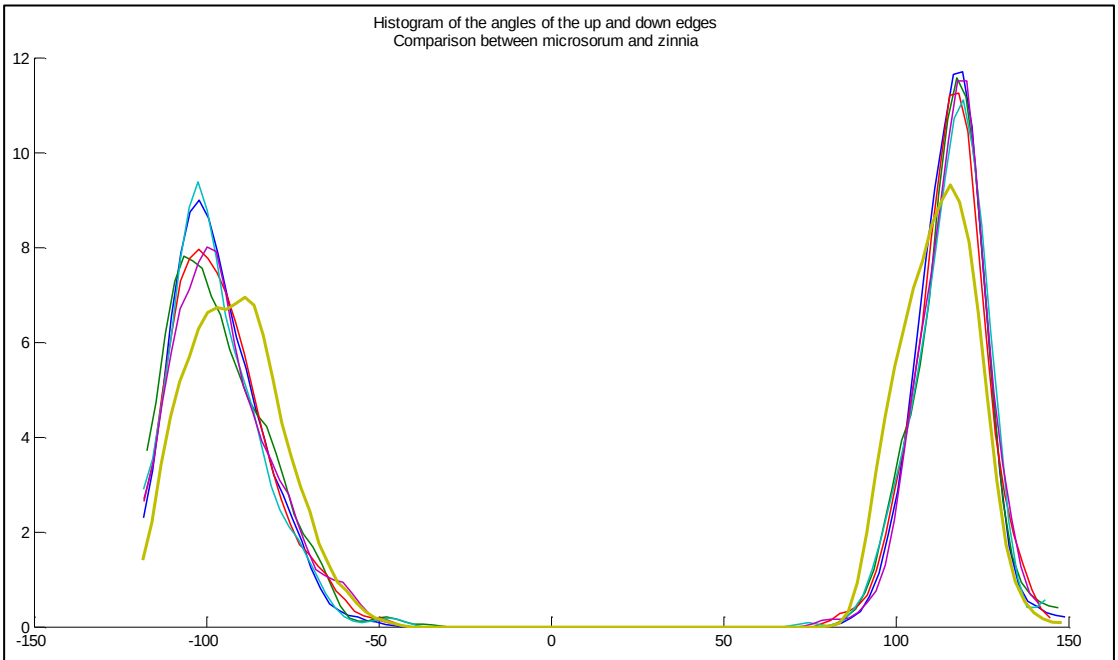

Figure 3. One statistical characterization of the plotedge technique

Here, we see the repartition in angles of the edges we have sorted and plotted. We can see from this graph that Zinnia tissue (thick yellowish representation) is "younger", and is really different from the Microsorum tissues.

1.IV. About histograms – functions ‘hist2’ and ‘histv2’

I want to present briefly two convenient pseudo-histogram tools that I have created and which could be very useful to anyone who want to make ‘smart’ histograms, revealing more accurately the trends we need to see. Indeed, in representing classic histograms, you need to make a compromise between the resolution in the interval-sampling of the set and the resolution of the measure of the distribution. One extreme example would be the histogram with two bins that counts with great precision what is the repartition of events below or above a certain value; its counterpart would be a histogram with a number of bins greater than the total range divided by the smallest distance between two values, taking values equal to 0 or 1. I faced this paradigm when representing the statistical repartition of the angles for the three edges, in the edge plotting method described above. I have a number of vertices plotted which is around 200, and I want to describe the behavior of the distribution quite finely, in an easy-looking representation, for comparing tissues. I finally used the function hist2, with selective smoothing. These two tools must be understood prior of using it, to avoid nasty effect on your results (hence reasoning).

1.IV.a Bin sliding histogram: ‘histv2’

This is the most intuitive declination of the classic histogram. It is the result of taking a bin that you ‘slide’ along the sample values: you compute the number of points in this bin on more points than if you had a classic histogram. You end up with a more precise description of your distribution. Below (Figure 5) is an example of a simulated random variable following the Gaussian repartition law. You can see that the bin sliding histograms give us a very good description of the sample, because we can have 50 points but for bins that are computed with the resolution in the mesure equal to the classical histogram with 10 points. For more precision about how to use `histv` and how it works, the reader is advised to look at the help section of the program copied in “Annex 1: help sections of programs.”.

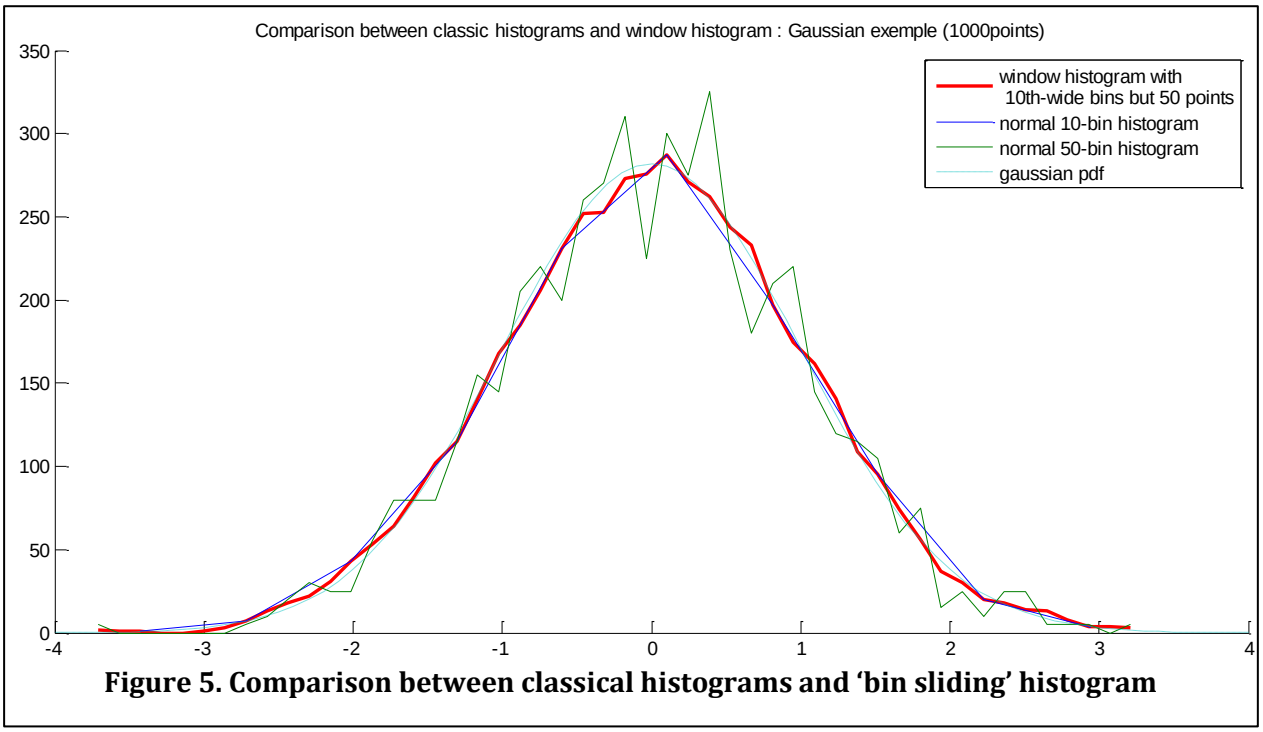

Figure 5. Comparison between classical histograms and ‘bin sliding’ histogram

1.IV.b Selective smoothing histogram: 'hist2'

This declination is trickier. Compared to a classic histogram, it computes each point by taking information from the bin of the considered value *and* the neighbor bins, with polynomial weights. It enables to get a histogram with small bins but getting rid of the fast variations of it. The help section of the program, which is copied in the annexes, gives great – and interesting – details about it. This tool is really powerful since it makes the histogram "speak" about the distribution, provided you know which trend of the histogram you want to shed light on (See Figure 6).

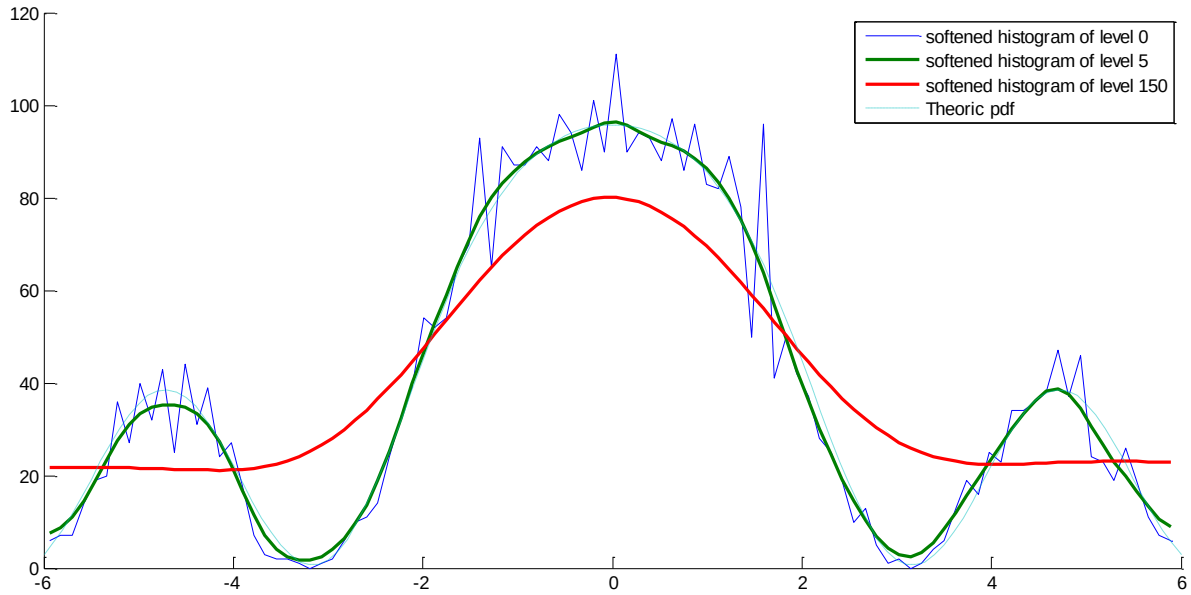

Figure 6. Comparison between classical and softened histograms with 100 bins

The set of 4000 points has been generated by a Monte-Carlo simulation, following a theoretical pdf created from a **Gaussian law plus a cosine**. We can see that different level of softened histogram cut a different range of variations.

2. Dividing tissues, faster

In order to do simulation concerning Errera's rules, we need to have a program that computes the planes that satisfy these rules. Moreover, this program should be fast since we want to do simulations on big tissues to have relevant statistical data. The aim would be to implement for the first time a complete model of growth *and* division of the cell for a complete tissue.

2.I. Start and aim

2.I.a Previous program

Sebastien Besson had already created such a program to compare real division and deterministic division following Errera's rules in order to shed light on the probabilistic behavior that we presented before. Nevertheless, this program was really reliable, but was also too slow. The computation time for a tissue of 200 cells was around 10 minutes, which is far too long if we want to test different types of simulation, for broader tissues, and along more generations than one.

This program works as an optimization along *two* dimensions. Let us consider two edges e_1 and e_2 between which we want to find the only plane that will divide the cell in two daughter cells with equal area, provided that this plane exists. The core calculus of the program is to find geometrically the arc of circle that intersects two given points O_1 and O_2 of e_1 and e_2 and divides the area in two equals areas. In the meantime, this 'calculus core' get the length of this arc of circle. Both operations are really simple and very fast. The slow part is the research of the plane p_E itself, product of the research of the minimum along the two dimensions that determine the locations of O_1 and O_2 on e_1 and e_2.

2.I.b The gist of the new program

It occurred to me that the old program did not take enough advantage of the precise characterization of the dividing plane. Actually, it can be easily verified that given a point O_1, there is only one plane that will be an arc of circle intersecting both edges e_1 and e_2 with right angles and starting from O_1. The challenge is then to find a way to implement the research of this plane, given O_1, but with a deterministic algorithm. Afterwards, an optimization on one dimension (the abscissa of O_1 on e_1), will find the plane that divide the cell in two equally sized daughter cells. The program that I get this way is almost 100 times faster than the previous one.

2.II. Geometrical core of the reasoning

The great challenge is to find a way to determine the position of 0_2 on e_2, given O_1, with a fast, deterministic method. The second step is to compute the area ratio between the two daughter cells defined by the computed dividing wall O_1O_2. It has been a bit long to find the proper geometrical method, and I will only briefly explain what is finally used in the program.

2.II.a Explanation of the main geometrical method

We are looking for the appropriate way to characterize the solution that will enable us to find the arc of circle that link edges e_1 and e_2 starting from a given point O_1 of e_2. Let's consider the drawing below:

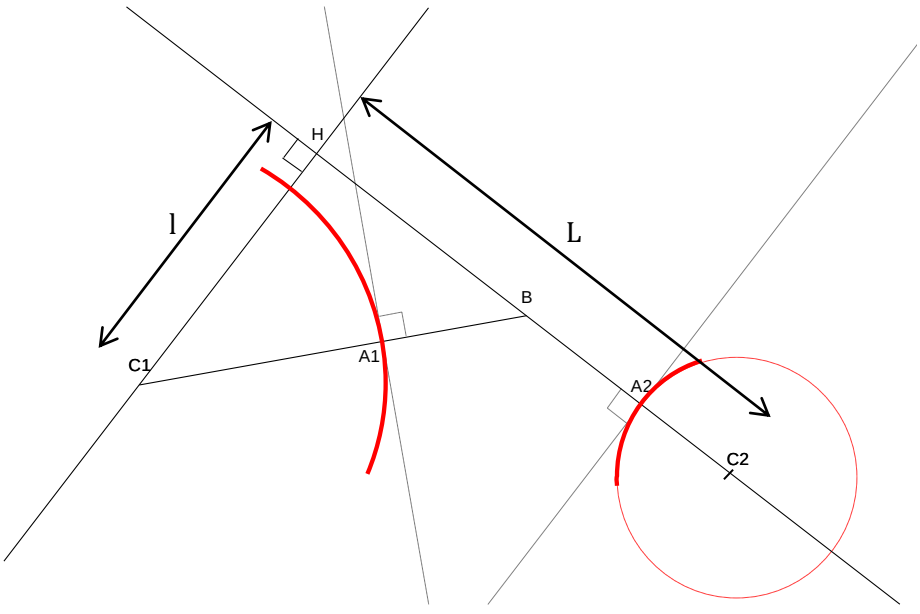

Figure 7. Drawing for explanation of the geometrical core of the division program.

The arc of circle edges are in bold red, our starting point O_1 is here A2, and the point that we are looking for is A1, such that A2A1 is an arc of circle which joins the two edges with right angles. (not drawn)

There are a lot of ways to characterize the solution, and we will use now:

$$A1B = A2B = r$$

I have drawn the right triangle C1HB which can be deterministically found, with the lengths L and l. In this triangle:

$$HB^2 + HC1^2 = BC1^2$$

i.e.:

$$(L - r2 - r)^2 + l^2 = (r + r1)^2$$

Which leads to:

$$r = \frac{l^2 - r1^2 + (L - r2)^2}{2 * \big((L - r2) + r1\big)}$$

With $r2$ the radius of the 'starting' edge and $r1$ the radius of the 'aimed' edge.*

2.II.b Generalization

Actually, this equation covers only the case represented in the drawing. We actually need to consider a oriented version of this token, with lengths oriented along each direction starting from the center of each circles. It leads to two results:

- The real equation (see MATLAB files) is a bit more complicated, in order to cope with the four types of cases we encounter. These four types differ from each other by the convexity of the arc of circles (convex or concave regarding the inner of the cell).
- The relation of Pythagore holds for any orientation of the three different lengths at stake, thanks to the fact that we compute square values. It enables us to get rid of any variation of the drawing within the four types.

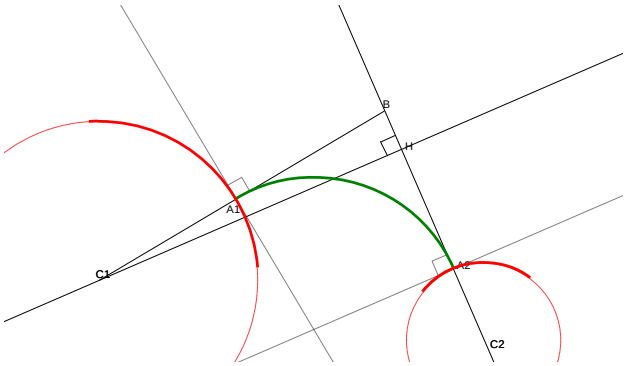

2.II.c Alternative method

Because in some extreme case (when L tends to be null), the calculus can pose some problem, I have added an exception which compute the solution with another geometrical method which is very reliable in these cases but slow and not reliable in general. This is actually the first method I

* As confusing as it may be, the aim is to stick with the notations of the graph, but the numbers are inverted in the written program. You will also note that the point 'B' is called 'R' in the MATLAB file.

implemented, and it is basically the equalization of the two length from the two points O_1 and O_2 to the center of the new dividing wall in arc of circle.

2.III. Explanation of the division program

Since the general method of this new division program is not the same from the previous one, I needed to design a new one from scratch. Here I provide an overview of how the Matlab files interact, and explanations of the different methods at stake.

2.III.a General structure

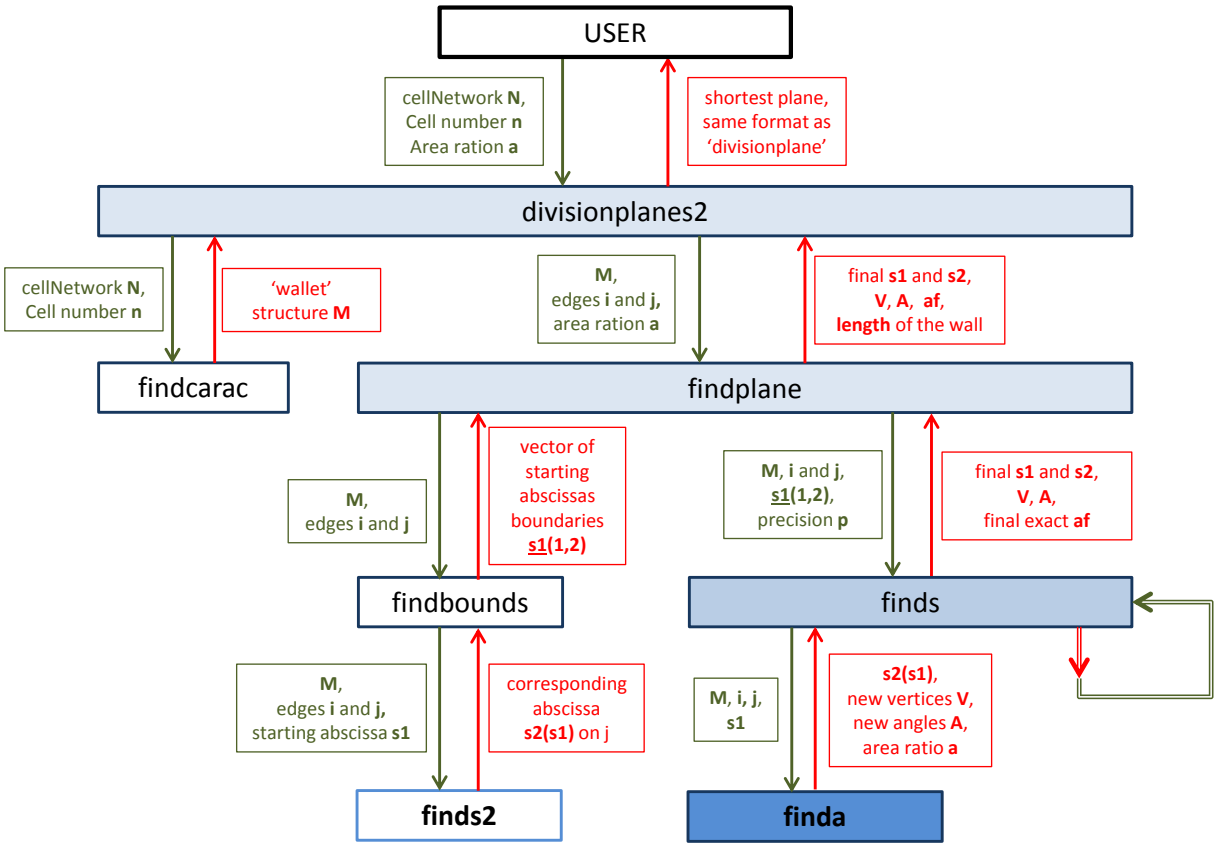

Part II:
Study of division on plant meristems

1. Abstract

1.I. Introduction

In order to test the predictive power of the division rules stated above, we must try to compare them to biological systems more and more diverse. Many studies have been carried out on epidermal, flat tissues but here we propose to expand these studies on a crucial area of the plant: the meristem. The meristem of plants is a very interesting zone to study, since it is the main area of division, featuring undifferentiated cells that divide at a constant and high rate. Yet, contrary to the epidermal tissues, these meristems are not planar tissue, but rather have shapes in between cone and hemisphere which vary from a system to another. We want to compare the shape of observed cells on these meristems with some shape that would be predicted by Errera's rules. We will use two different approaches, one analytical research of key solutions, and one numerical approach with simulation relying on the division program we developed on Matlab.

1.II. General method

To carry out these comparisons, we will assume that a good representation of a meristem is a perfect cone, and we will focus on the central cell, which is at the heart of the division process. The cone approximation enables us to do all calculation of length and area on a diminished 2D plane. This 2D plane is the result of cutting the cone along a generating line and laying it on a flat surface. We will use the angle gamma of the resulting 'forbidden area' on this 2D plane to characterize the cone. The relation between this angle gamma and the geometrical angle of the cone is illustrated on Figure 8. I will only detail in this abstract the first step, i.e. the analytical approach.

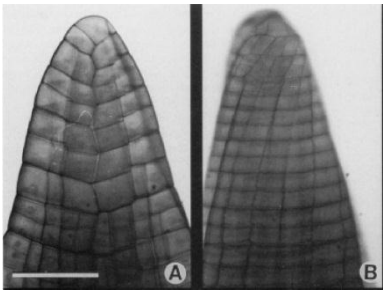

Figure 9. Example of pseudo-conic meristem with the Funaria apex

Figure 8 Relation between the 2D-gamma plane used for computation and the real cone

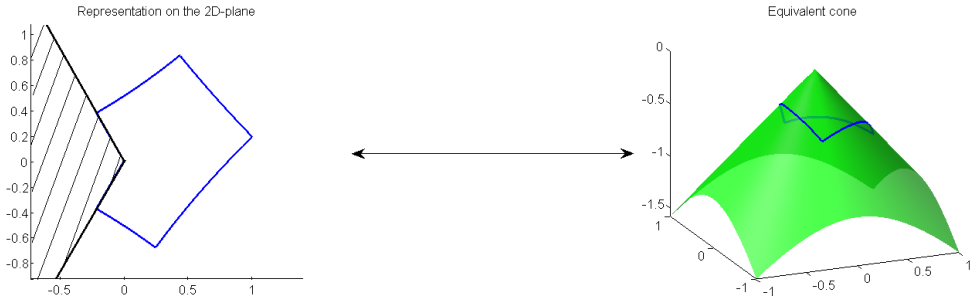

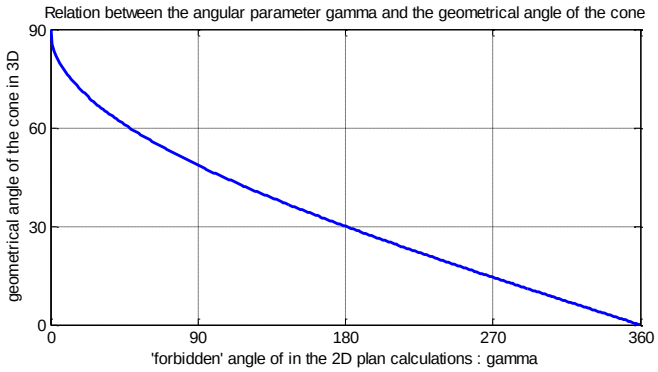

1.III. Fixed point solution on the cone

This analytical approach consists on finding cell shapes that satisfy some hypothesis which characterize the division on the center of meristems. Since a meristem can undergo between n and n REF division during its characteristic period of growth, the cell shapes that we observe are the result of a great number of these divisions. We will therefore look for 'fixed-point' solutions of the dynamic system defined by the central cell of the meristem, undergoing transformations that are framed by two major hypotheses. We want to figure out analytically what these solutions could be, and see how the shape of these solutions change with the parameter of the cone, gamma.

The *first hypothesis* is the fact that on the center of meristems, the growth between divisions is isotropic: shapes of the cells don't change between two divisions, only the characteristic length increases. The *second hypothesis* is the fact that the division which occurs on the center of this cone follows non-deterministic Errera's rules: the plane of division has the Errera shape, and the area of the mother cell is divided by two. Within the framework of these two hypotheses, we decide to look for solutions that are 'fixed-point solutions' *in one step*, which are preserved by one division and growth process. This has direct implications that are very useful to determine the solutions:

- The cell itself is made of walls that are products of previous divisions, whose shape is not altered during growth. Therefore, the walls of the cell are all arc of circles that connect each other with right angles ("Errera shape").
- Since growth is isotropic, the division should produce one of the daughter cell with the exact same shape than the shape of the mother cell. The self-similar daughter cell has half the area of the mother cell.

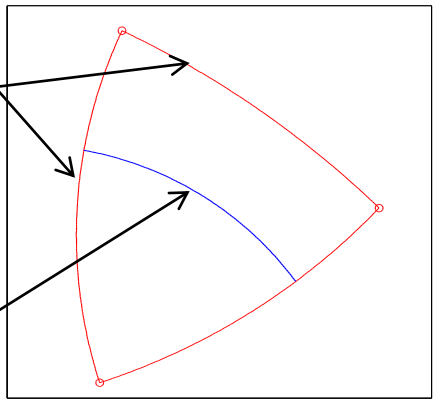

These two constraints define exactly our problem of "fixed-point solution on the cone" of which we seek the solutions. The interested reader is advised to have a look at the chapter 2 and 3 of this part to grasp thoroughly the concepts behind this research.

1.IV. Results

Having defined the proper geometrical parameters to describe the cell shape and set the right geometrical constraints that translate these hypotheses, we can implement a numerical resolution of our simple equations (see Section 2 of this part). These different solutions are then represented on the cone after proper transformations that enable us to jump from the 2D plane to the real cone. All these tasks are performed by a Matlab set of functions and scripts presented in the section "*3.Explanation of the resolution process*

Documentation of Matlab program". The first important result is the quasi-uniqueness of solution per number n of edges of this solution and per value of γ, the parameter of the cone. For each value of n and γ, there is no more than two solutions ($*$ 2 with the axial symmetry) if we consider the shape of the cell (size of the cell itseld and orientation around the cone may change).

1.IV.a Shape of solutions

The main results are the shape of the solutions depending on gamma, for any number of edges of this solution. There are two different solutions with five edges, one solution with 1 to 4 edges, and there is no solution with more than 6 edges for positive values of gamma. These positive values of gamma define a cone whereas negative values of gamma define a shape that can be interesting for some application but are not tackled yet - even though the computations remain valid for gamma< 0.

The results have been gathered into a dynamic GUI (Graphic User Interface) that can be provided upon asking†. This GUI displays in 3D the fixed-point solutions of the division problem for cells from 2 to 5 edges. These solutions do not exist for all values of gamma, and their existences are limited by a maximum value of gamma, which decreases with the number of edges. (see Table 1: "Geometric limitations and Existence domains of the cell shapes regarding the parameter gamma of the cone"). Several of these shapes are shown below.

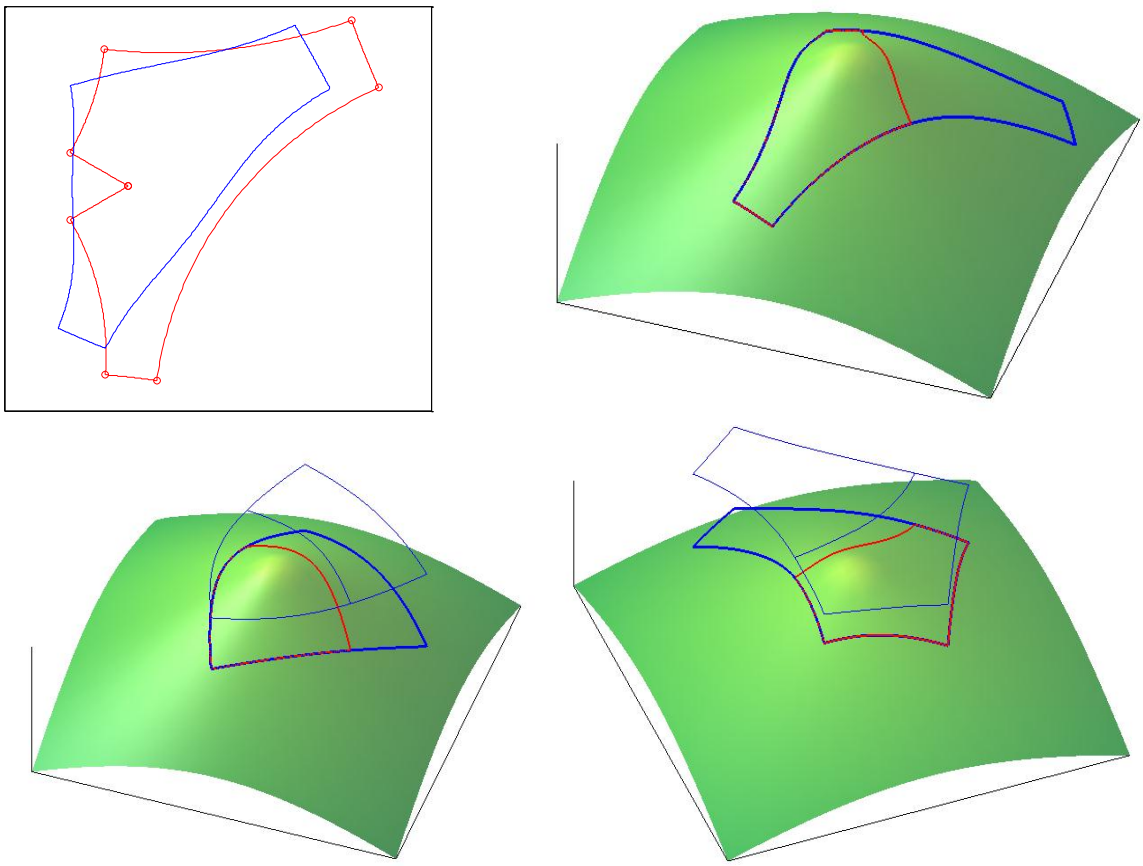

Figure 10 Examples of 3D shape of the solutions

From upper left to bottom right: 2D representation on the gamma plane of the solution shape for γ=60° et five-edged cell Type 2 (red line = as the result of the resolution; blue line = stretched for the projection on the cone); 3D representation of the latter; 3d representation with projection and dividing wall of 3 edged cell on a cone with γ=60°, and the same representation for γ=30 and a five edged cell Type 1.

† Upon asking the creator and writer of this prose at antoine.lizee@polytechnique.edu or the contact and supervising professor, Jacques Dumais, at jdumais@oeb.harvard.edu). The M-files of the GUI are working on any recent version of MATLAB. They may be included in the numerical package containing this report.

1.IV.b Existence domains of the solutions

The knowledge of the complete shape of the different solutions enables us to do the analytical computation for the research of the transition angle that would discriminate the existence domain of each solution. Indeed, the cell shapes that we have found are not complete solutions of the problem, since they are not necessarily the result of the optimal division of themselves. Indeed, even if the division plane which leads to an auto-similar daughter cell follows the general rules of divisions (arc of circles + right angles), it is not necessarily the shortest division plane among the candidates. "Self-stability" of the solution is granted when the deterministic cell division leads to the auto-similar daughter.

Instead of long exact analytical computation, I have chosen to take advantage of the strong division program which computes the possible division planes of a given cell (see Part I, section 2 of this report). This highly reliable program can compute with a great precision the geometrical characteristics of all the division planes; therefore, we are able to compute these limit angles for which there is a division plane that become larger than the one which lead to the auto-similar daughter cell. These results are summed up in below.

Shape of the cell	Gamma max (Geometrical limitations to self-similarity)	Existence domains ("self-stability" of the solution)
1 edge	360	234.5 / 360
2 edges	321.0	164.7 / 279.4
3 edges	266.7	- / 228.6
4 edges	187.3	-/ 135.5
5 edges	92.8	-/ 37.3
5 edges Type 2	133.0	- / 25.5
6 edges	-9.3	
7 edges	-114.0	
7 edges Type 2	-40.9	

Table 1 Geometric limitations and Existence domains of the cell shapes regarding the parameter gamma of the cone

These valuable results should be compared to numerical simulations, which will be able to describe the dynamic properties of the system. Indeed, these transitions values are strict boundaries in gamma that cannot be exceeded by the solution of interest, because a greater or smaller gamma would led the system to another cell shape. Nevertheless, this domain of existence for the solutions could never be reached by real systems. Division process from other cell shape could lead to solutions (like periodic ones, with different shapes alternating) that would not allow to 'drop' on the solution we have considered. This issue must be tackled by complete simulations I did not have the time to carry out.

We can go further in the discussion around these solutions and their use for understanding real division, and this discussion is developed in Section 4 below.

2. How to get to grips with the analytical finding of solutions on the cone

In this section, I try to provide the reader some elements to grasp easily the complexity in the resolution of this simple problem. I have personally been through different examples "hands-on" (2-edeged-cell, 3-edged cell on the complete plane), but they would be long to present here, and I will directly explain the proper way to solve the problem that embrace all the solutions, regardless the shape of the cell.

2.I. Explanation of the geometrical problem

If it is not already done, the reader is advised to read the section '1.III Fixed point solution on the cone' not to miss the starting point.

2.I.a Periodicity

The first important thing to understand is the periodicity implied by the first hypothesis within the framework of a fixed point solution. Regardless the aspect of the edges, the isotropic growth imposes that the daughter cell which have the same number of edges has also the exact same shape. Since n-3 edges are strictly preserved and 2 other edges have many characteristics in common, the shape of the mother cell is already very constrained, as shown in Figure 11.

2.I.b Semantic rotations

In addition, we know that every edge must be shrunk by a $\sqrt{2}$ ratio during the division, because the final area in the daughter cell is half of the area of the mother cell. This leads to a more accurate definition of the geometrical consequences of our hypotheses. Indeed, the periodicity is not only needed, but every edge must be accounted in this periodicity, because if one edge is left behind in this process of transformation, it cannot be shrunk and keep the same shape at the same time – except for the straight edge exception.

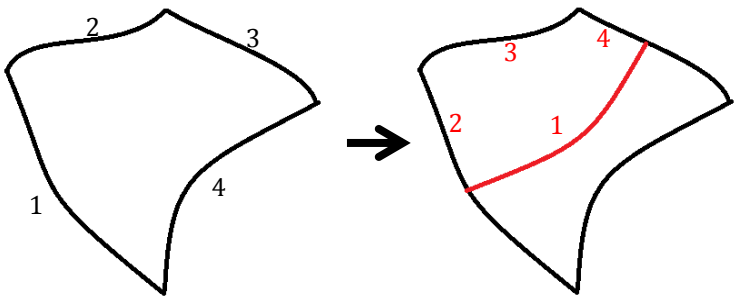

Numbers label edges. Black numbers label edges in the mother cell, red numbers label edges of the daughter cell.

Considering that the new wall (red) have the role in the daughter cell that the wall "1" had in the mother cell, all the walls are rotated to preserve the global shape between the mother and the daughter cell. A lot of constraints arise concerning the shape of the mother cell. For instance the wall 2 should have the exact same shape of the wall 3, with only a difference in size – which is obviously not the case in this example.

Figure 11. Illustration of the constraints that stem from cell division with a dummy example

This periodicity should be understood deeply, through the concept of the "semantic rotations" that could occur to the edges during the division. Let see that with examples: in the four edges case we have two possible "semantic rotations". The first one, represented in Figure 11, can be described as follow: edge number 1 of the mother cell takes the role in the daughter cell that edge number 2 had in the mother cell, edge 2 takes the role of edge 3, edge with role number 4 in the daughter cell is located on the edge 3 of the mother cell, and edge 4 is replaced by the new

edge, as a result of the division, which take the role of edge 1. If each arrow "->" means "becomes", this semantic transformation can be summed up with this formula:

$$1 \rightarrow 2 \rightarrow 3 \rightarrow 4$$

whereas the representation of the other semantic rotation can be summed up by:

$$3 \rightarrow 2 \rightarrow 1 \rightarrow 4$$

The second transformation is the symmetric of the first one, so we will only resolve the problem for transformation characterized by increasing numbers of edges, and the solution could be flipped to get another solution, which is quite natural. Let us see right now why the semantic rotation of "Type 2", obtained by skipping one edge when rotating, does not lead to an self-similar daughter for the 4-edged cell. The formula would be:

$$1 \rightarrow 3 + 2 \leftrightarrow 4$$

the old edge 3 being replaced by the new edge, which has the role of edge 1. This is not an acceptable transformation, because the edges number 2 and 4 are flipped in their roles during the division. After two divisions, the edge which has been number 4 must have again the same shape has it has before, but with a smaller size. This is only possible for few shapes of edges, and on the particular case of arc of circles, only the straight edge could satisfy this paradigm (but anyway arise other problems). In the Type 1 rotation, all the edges become at one time the dividing wall and have the chance to completely change before they will have to assume again the role they had once before.

On the contrary, cell with odd numbers of edges beginning at 5 can undergo a semantic rotation of Type 2 during the division process. For instance, five-edged cells can undergo these two semantic rotations:

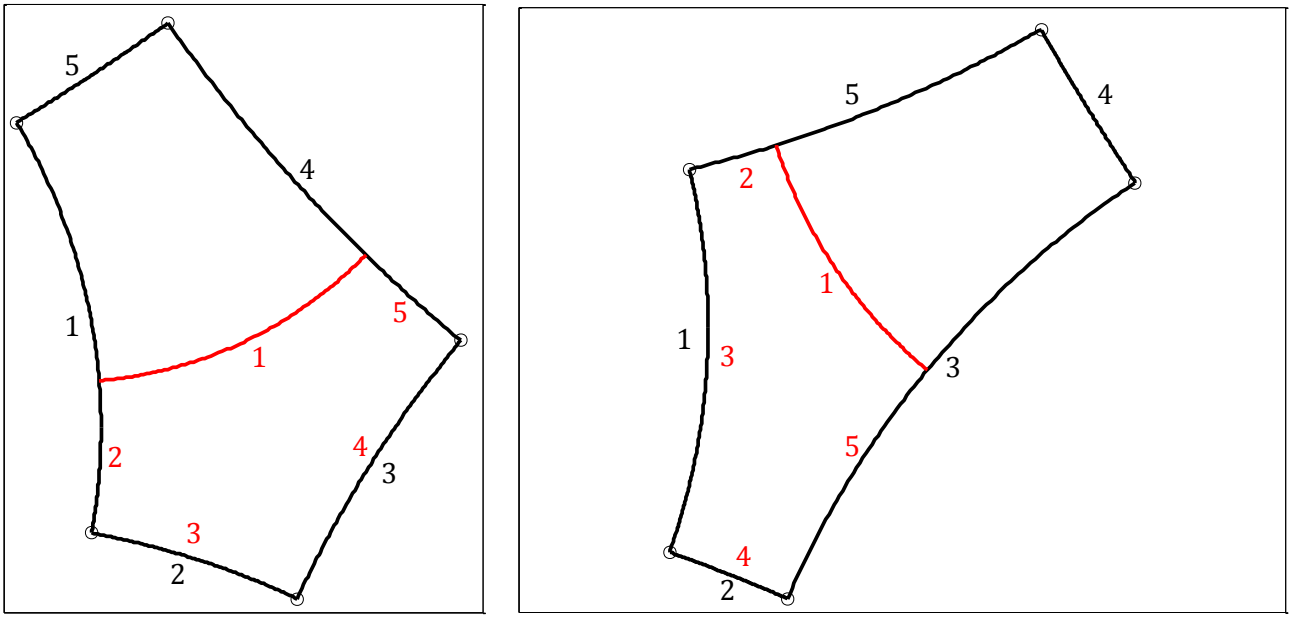

Figure 12. Difference between the Type 1and Type 2 semantic rotations with the 5-edged example on the complete plane (γ=0deg)

$$1 \rightarrow 2 \rightarrow 3 \rightarrow 4 \rightarrow 5 \text{ and } 1 \rightarrow 3 \rightarrow 5 \rightarrow 2 \rightarrow 4.$$

In the first transformation, of Type 1, the edge number 5 is replaced by the dividing wall whereas in the rotation of Type 2, the fourth edge is replaced. You can see both examples of rotations in Figure 12.
We have gathered all the different rotations that could be undergone during a division by a solution cell in the following table. We have kept only the transformations that are not redundant with the symmetric transformations of lower rotations. For instance, the Type 2 rotation in a 3-edged cell equals the "Type -1" rotation – which is the symmetric of the Type 1 rotation. It is eventually basic algebra. To get all the possible solutions of the problem, we should determine all the shapes of the solutions for each possible transformation, depending on the number of edges of the final solution we want to get. Fortunately, we will see that there are no more than a few solutions for a cone, which are limited in their number of edges.

Number of Edges	2	3	4	5	6	7	8	9	10	11	12	13	14
Type	1=-1	1	1	1,2	1	1,2,3	1,3	1,2,4	1,3	1,2,3,4,5	1,3,5	1,2,3,4,5,6	1,3,5

Table 2. Existing Types of semantic rotation that could be undergone by the cell during the division, and which are not redundant with symmetric rotations.

The first important result is already at hand: if we make the hypothesis that each semantic rotation leads to only one solution (plus the symmetric), there is no more solutions than the number of semantic rotations. This hypothesis can be proven right now but we will prove it anyway through the resolution of the problem.

2.II. The good set of parameters

From each semantic rotation stem relations between the edges. These relations should characterize the shape of the mother cell, and give us the solution we seek. We do not know now if the geometrical constraints set by the definition of the semantic rotations are strong enough to determine one solution for each angle, nor do we know whether there will be a solution for each angle – a cell with a shape that will satisfy the relations set by the semantic rotation we consider. Nevertheless, we know that this transposition, from the isotropic growth hypothesis to the relations between edges imposed by the semantic rotation, is lossless in terms of constraints.

Let us see an example of what these relations are. If we consider the resolution of the problem for the 4-edged cell, there are only two set of solutions, one being the symmetric of the other. Considering the Type 1 semantic rotation give us all the solutions. Concerning the solution of this rotation, and minus the $\sqrt{2}$ ratio, we know that:

- all the characteristics of the edge 2 are these of the edge 3
- some of the characteristics of edge 1 are inherited from edge 2
- some of the characteristics of edge 3 are inherited from edge 4

We still need to add one last element to get the full equivalent of the perfect division problem: the edges have Errera shape. They are all arc of circles. Thus we need a good parameterization of the edges in order to translate the relations between them efficiently. The major challenge concerns the 3 edges that change partly (the new one, and the two adjacent), whereas the n-3 others are strictly preserved. We want the parameters which will characterize these 3 edges to change the less possible. In addition, these parameters must locate the cell regarding the center

of the cone, which is also the center of the gamma plane. After many examples and trials, I found the golden set for each edge:

- R_i The radius of curvature R_i is strictly maintained between the edges, regardless they are cut or not during the division. The $\sqrt{2}$ ratio is directly multiplied to R_i. This is the most convenient and obvious parameter.
- h_i The distance hi from the center of the center to the edge has also the precious characteristic to be kept when an edge is cut in parts. The $\sqrt{2}$ ratio is also directly multiplied to h_i.
- θ_i We need now to locate these edges around the point. Therefore, the choice of hi impose to take as the third parameter for each edge the angle between the segments $[h_i]$.

This set of parameter is sufficient to completely define the solution, and the entire set is needed.

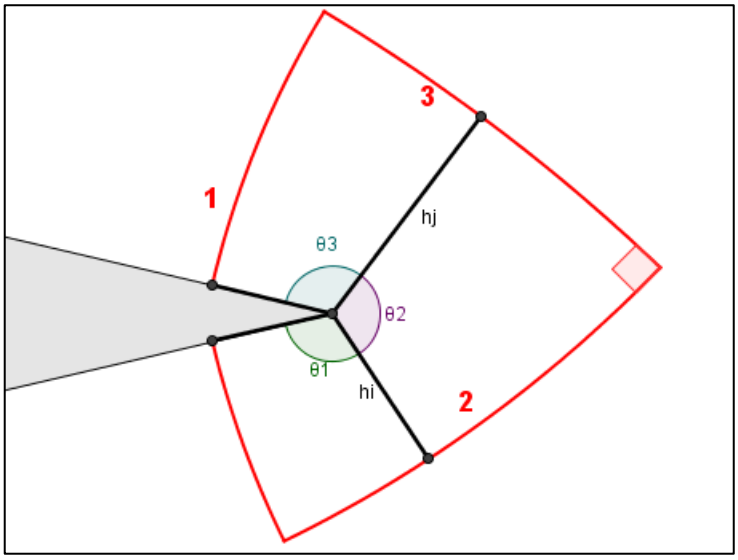

Figure 13. Illustration of the parameters h_i and θ_i

The black segments are the shortest distances between each edge in arc of circle and the center of the cone. These segments intersect the edges with right angles and will not change if an edge is cut. They define the distances h_i. In this case 'h_i' and 'h_j' are the first and second distances that define the second quarter between edge 2 and edge 3 (see next) but they should be named 'h_2' and 'h_3'.

2.III. Summary of the steps of reasoning

I try to summarize in the following figure the path we took throughout this section and the sub-section *"1.III Fixed point solution on the cone"*.

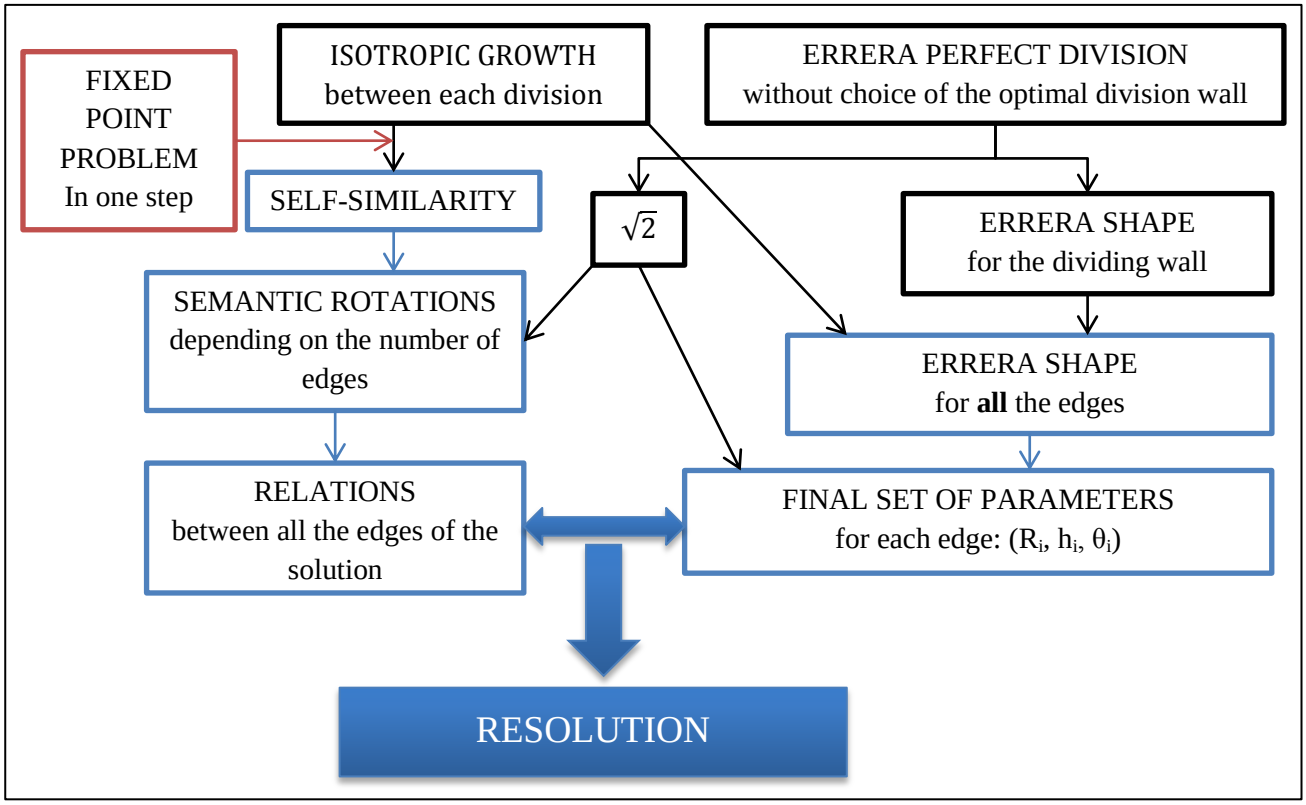

3. Explanation of the resolution process

Documentation of Matlab program

Provided the good set of parameters to describe each edge of the solution, provided the relations between all the edges, we must now carry on the resolution of the problem, with the aim of seeing and handling the solutions easily. In this section, I will describe the different steps carried out by my MATLAB program to solve the problem and then display it. It is the documentation that must be provided in order to fully understand the organization of the MATLAB program and the role of its components. In addition, the computing reader must refer to the lengthy help sections located at the beginning of each function of the program.

3.I. Birth of the geometrical quarters of resolution

We can now express the relations in the set of parameters we have chosen. We first draw the segments [h_i] which link the center of the cone and the edge with the shortest distance. These segments are therefore attached to the edges with a right angle, as shown in Figure 13. They define quarters that will help us to get the final solution. We will go through the two main cases of Type 1 and Type 2, to show that this resolution process is a general method.

3.I.a Type 1 case

Let us consider the five-edged case. The formula to describe the Type 1 division process and the related semantic rotation of the edges would be:

$$1 \rightarrow 2 \rightarrow 3 \rightarrow 4 \rightarrow 5$$

Given the conservation properties of the radius R_i, we can infer:

$$R_2 = \sqrt{2} * R_1$$
$$R_3 = \sqrt{2} * R_2 = 2 * R_1$$
$$R_4 = \sqrt{2} * R_3 = 2\sqrt{2} * R_1$$
$$R_5 = \sqrt{2} * R_4 = 4 * R_1$$

We get a similar result for h_i, because this parameter has the same properties of conservation (no change from an edge to a 'daughter' edge located on the previous one) and size modification (multiplication by $\sqrt{2}$ of the parameter for the daughter cell with half the area) compared to R_i:

$$h_i = \sqrt{2}^{i-1} * h_1$$

Concerning the θ angles, we must consider not only the length but the segments $[h_i]$, and we can see that only the angles around the new segment "$h_{1'}$", corresponding to the new dividing wall, change during the division process. To mark this, we will use the notation " ' " to denote the parameter of the edge in the daughter cell. By convention, θ_i is the angle between $[h_i]$ and $[h_{i+1}]$. The size modification for the theta angles is 1, and the angles that have similar roles between the mother and the daughter cells must have the same values. We get:

$$\theta_{i'} = \theta_i$$

Then:

$$\theta_{2'} = \boxed{\theta_1 = \theta_2}$$
$$\theta_{3'} = \boxed{\theta_2 = \theta_3}$$
$$\theta_{4'} = \boxed{\theta_3 = \theta_4}$$
$$\theta'_5 \neq \theta_4$$
$$\theta'_1 \neq \theta_5$$

This gives the definition of two angles θ_A and θ_B, and these relations do not depend on the number of edges. Actually, we see emerge two different quarters, A and B, at the heart of the cell. All the n-1 quarters defined by $[h_i]$ and $[h_{i+1}]$ for i=1…n-1, are all similar within a size difference‡. They are the quarters of Type A whereas the quarter of Type B is only found between the two extreme $[h_n]$ and $[h_1]$. All the divisions of Type 1 have only these two Types of quarters, both of them with the same structure. The root of the differentiation between these two Types of quarters is the ratio r between the two lengths of the segments that define them. As a convention, we take the values for r that are greater than one, which implies that we flip the Quarter of Type B. In the Type 1 rotations we have:

$$r_A = \sqrt{2}$$
$$r_B = (\sqrt{2})^{n-1}$$

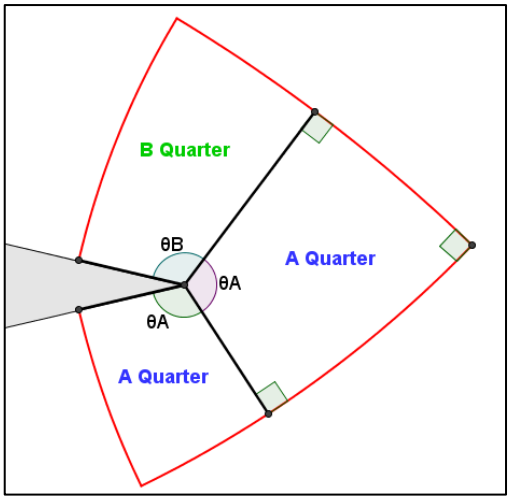

Figure 14. Displaying of the two Types of quarters for a cell with n=3

‡ The fact that the quarters are auto-similar comes from the shared angle θ, the shared ratio r, and the other properties that define a quarter (right angles, radius of the edges proportional to h, arc of circles).

Now that we have reduced the problem to these two quarters, we see finally how we have reached some general resolution of the problem, since it does not depend on the number of edges nor the angle gamma. These two constraints just impose the following relation, which link the two angles we need to determinate:

$$\gamma = 2\pi - (n-1) * \theta_A - \theta_B$$

3.I.b Type 2 case

The Type 2 semantic rotation is represented by:

$$1 \to 3 \to 5 \to 2 \to 4$$

Being this time the edge 4 which is replaced by the new edge. This led to these relations by a similar token than before:

$$R_3 = \sqrt{2}R_1$$
$$R_5 = 2R_1$$
$$R_2 = 2\sqrt{2}\,R_1$$
$$R_4 = 4R_1$$

With similar relations for h_i. By drawing Figure 15, we see now that we can extend our resolution implying two Types A and B of quarters to the semantic rotation of Type 2, and actually to any semantic rotation of Type N. We must only change the ratios r_A and r_B which defines the two quarters. Here we have:

$$r_A = \left(\sqrt{2}\right)^{E\left(\frac{n}{2}\right)}$$
$$r_B = \frac{r_A}{\sqrt{2}}$$

Which for five edges gives: $r_A = 2\sqrt{2}$ and $r_B = 2$.

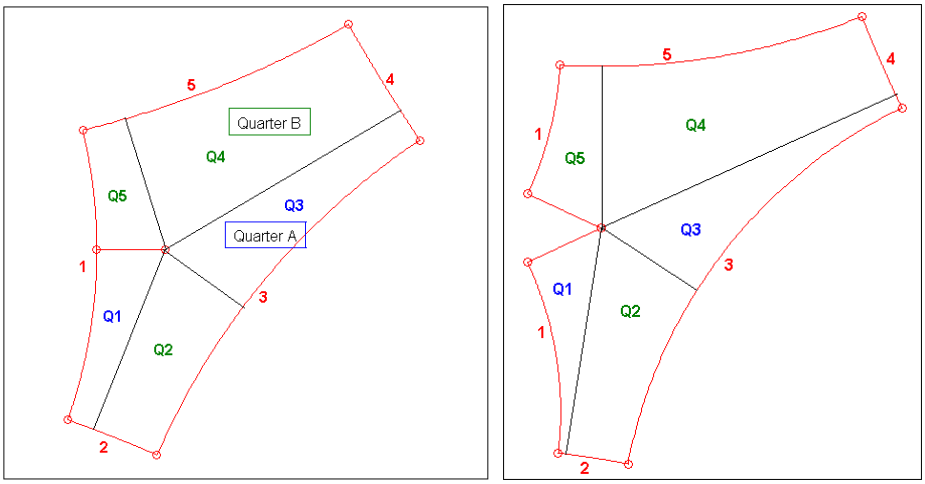

Figure 15. Quick draw of a 5-edged solution to a Type 2 rotation

The first draw is for γ=0° (full plane) and the second for γ=50°.
$[h_1]$ is in red whereas the other $[h_i]$ are in black. The B Quarters are written in green, the A quarters in blue.
Let us notice that the size of the segments $[h_i]$ increases by step of $\sqrt{2}$ with skipping one each time.

3.I.c What next? Summary

We have reduced the problem to these two different quarters. Before going further, we need a little recap of what we know about the cell. As seen just above, the semantic rotation gives us a lot of information on the set of parameters, combined with the particular geometry of the cell. If we set R_1=R as the value for normalization of the figure, we know:

R_i We know all the values of $(R_i)_{i=1\dots n}$ from R_1.

h_i We know with similar relation all the values $(h_i)_{i=1\dots n}$ given h_1. Actually, for $i = 1 \dots n$, we know that $h_i = R_i * \delta$, because the relations that link the (h_i) family and the (R_i) family are exactly the same. Thus, we will use δ instead of h_1 as the unknown parameter to get the values of $(h_i)_{i=1\dots n}$.

θ_i We know that there are only two different values: θ_A and θ_B. But we know that these two unknowns are related by the equation:

$$\gamma = 2\pi - (n-1) * \theta_A - \theta_B$$

There is now only two unknowns left: δ and θ_A(or θ_B). We know that the rest of the information we need lies in these two quarters we have defined, and particularly in the structure of these quarters: the right angles and the edges in arc of circles.

3.II. Global sketch of the resolution

The figure presented here shows all the steps of the resolution. You see in the blue frames the working variables, and in red frames the functions that handle them.

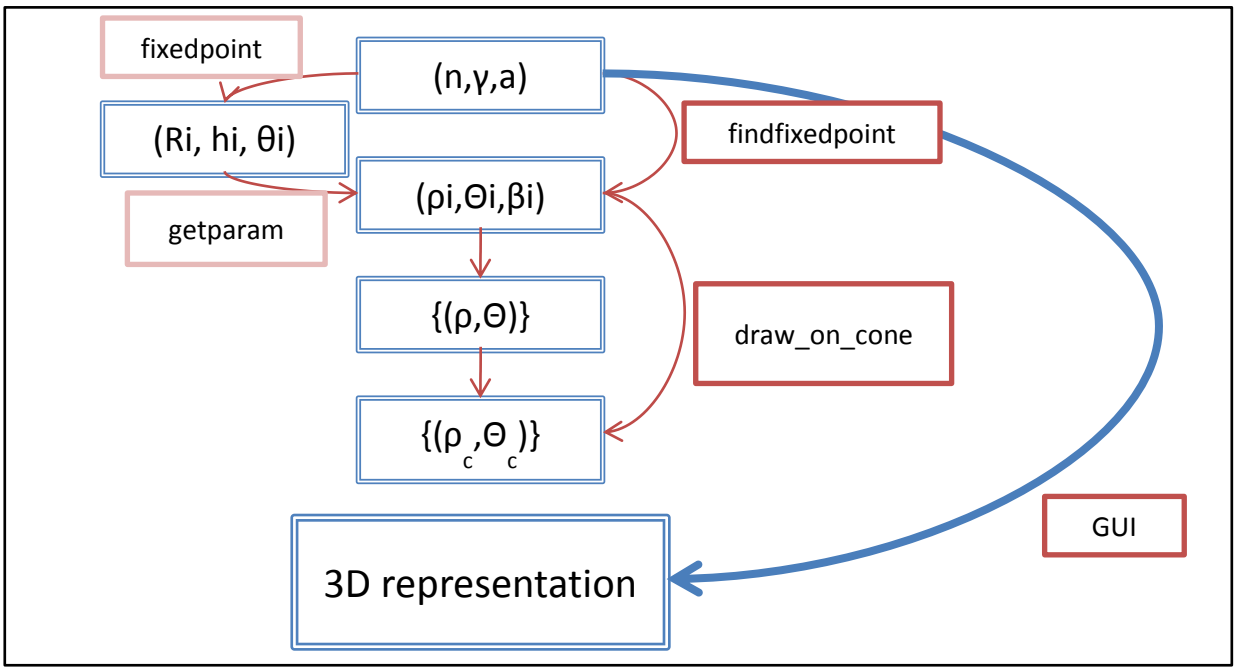

Figure 16. Global sketch of the resolution

3.III. Details of the resolution process

3.III.a Core resolution

The core resolution consists on the finding and characterizing the solution. Granted n, the number of edges, gamma, the angular parameter of the cone, and a, the normalizing area, we must find some values that entirely characterize the shape of the solution. This work is done by '`fixedpoint`', which solve equations in the working set of parameters (Ri, hi, θi) we have discussed above. This resolution takes its roots in the two quarters A and B that are defined by

the drawing of the segments [h_i]. As stated above, we only need to determine the two unknowns δ and one angle θ. We need one equation by quarter, and this equation lies in the figure below.

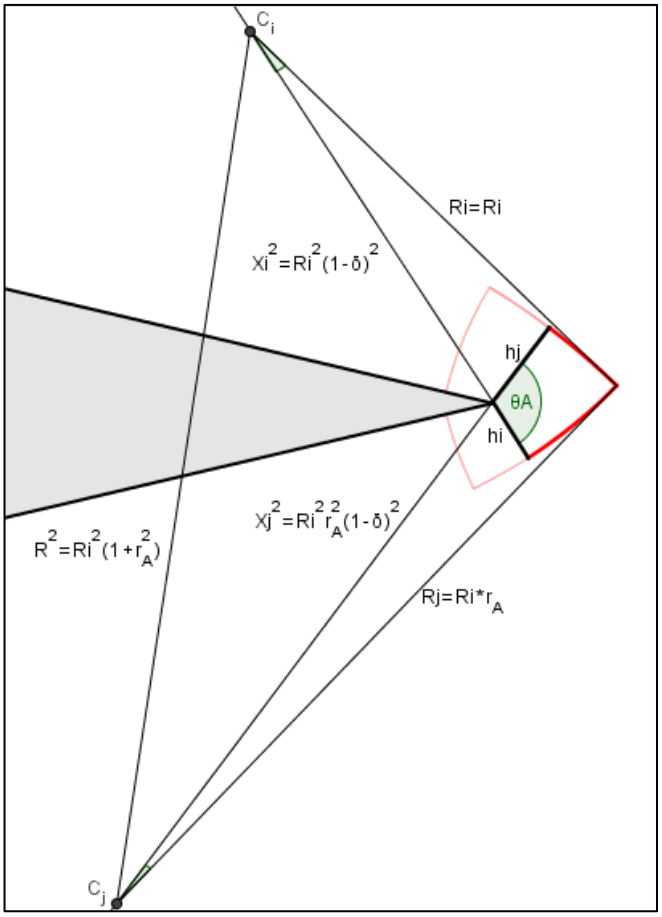

The outer triangle is a right triangle, coming from the fact that the edges of the cell intersect with a right angle. This gives us a first relation:

$$R^2 = R_i^2(1 + r_A^2)$$

Afterwards, a simple Al Kashi formula applied to the inner triangle leads to the relation we are looking for:

$$R^2 = X_j^2 + X_i^2 - 2X_iX_jcos\theta_A$$

Soit, en simplifiant par R_i:

$$(1 + r_A^2) = (1 - \delta)^2(1 + r_A^2) - 2(1 - \delta)^2 r_A cos\theta_A$$

$i.e.$:

$$(1 + r_A^2) = (1 - \delta)^2(1 - 2r_A cos\theta_A + r_A^2)$$

Finally:

$$\boxed{\delta = \sqrt{\frac{1 + r_A^2}{1 - 2r_A cos\theta_A + r_A^2}}}$$

With r_A given by the semantic rotation we consider, this is a relation that we can write as: $\delta = f(\theta_A)$. Applying the same token to the B quarter give us the exact same relation $\delta = f(\theta_B) = g(\theta_A)$ using the relation we know between θ_A and θ_B. Resolving the system gives us all the values for the entire set of parameters (R_i, h_i, θ_i).

3.III.b Transformation of the set of parameters

We must note that the working set of parameters leads to the complete solution, since it enables anyone to draw the solution with a ruler, a compass and a measure of angles. Nevertheless it is not really convenient for computer drawing or analyzing of the shape. Thus, we need to get the solution in another set of parameters, which is basically the set used to describe any cell in the cellNetwork environment: the vertices coordinates (here, polar) plus the angles between the cord lengths and the curved edges. This particular task is carried out by the '`getparam`' function, which is used in the broader '`findfixedpoint`' function that give the solution in the convenient set of parameters from the input of n, gamma and a. '`findfixedpoint`' uses both '`fixedpoint`' and '`getparam`'.

3.III.c Displaying of solutions

Given the final values to describe the cell which is the solution of the problem, we need to put it back on the cone on two steps. First we will numerically create a big number of points to "map" the boundaries of the cell, translating the curvature in a big set of polar coordinates which

describes the edges. Then we will "close" the gamma plane by to recreate the cone. This is done by a simple transformation described by the following equations:

$$\begin{cases} \theta' = \theta * \alpha \\ r' = \dfrac{r}{\alpha} \\ z = r * \sqrt{1 - \dfrac{1}{\alpha^2}} \end{cases}$$

With:

$$\alpha = \frac{\pi}{\pi - \frac{\gamma}{2}}$$

After setting up some visual elements and drawn the cone, we can display it in a nice 3D window of Matlab, to observe it accurately. REF is a snapshot of what is the result of this resolution process.

In order for the final user to easily get and manipulate these solutions, I have developed a GUI (Graphical User Interface) that displays dynamically the solutions for any angle and any number of edges. I have not yet succeeded in making this GUI portable and not platform dependent as a standalone application, but the Matlab files are available upon asking§.

3.IV. Remarks on the limitations of the resolution process

3.IV.a Geometrical limitations

We could spend a few lines and a figure to see why there are geometrical limitations to the existence of the solutions. The greater the number of edges, the harder it is to "fit" all these edges on the gamma-plane with the constraints, and particularly with the asymmetry needed for our problem of "growing self-similarity" between the edges. Below is several limit forms of these geometrical limitations. The limit angles displayed in Table 1 are computed numerically, using my drawing algorithm for any parameter gamma.

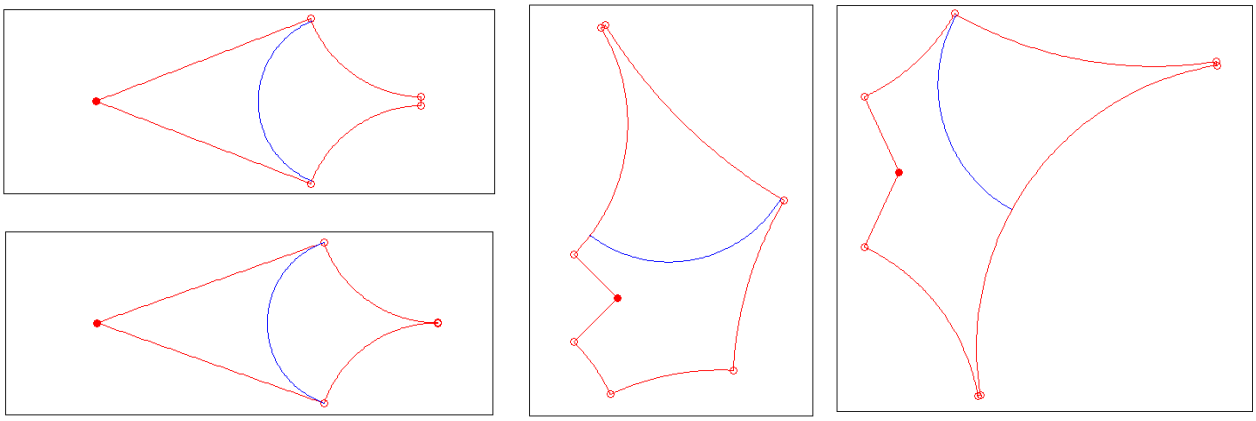

Figure 17. Different examples of geometrical limitation of our solutions.

From left to right: 2-edged solution for γ=318°, and limit solution at γ=321°; 5-edged solution of Type 1 for γ=90° (γ_{limit}=92.8°); 5-edged solution of Type 2 for γ=130° (γ_{limit}=133°). In blue is the dividing wall.
We can see on these examples that the edge which is the farer from the center get more and more shrunk to satisfy the problem. The limit shape is when it does not exist anymore, and there is no more right angles. Two (or more) different edges disappear simultaneously for the Type 2 solutions, because one is "left behind" during the division.

on any recent version of MATLAB. They may be included in the numerical package containing this report.

3.IV.b Computational limitations

The MATLAB program is fully functional, even for negative values of gamma, as shown in Figure REF. These values could be really interesting for the study of surfaces that are "saddle like" and which would be the transformation of a gamma-plane with negative value of the parameter γ. The resolution process and the computation are therefore really robust, they do not change for values of γ, or between convex and concave shapes (which is not obvious). Nevertheless, it exists one fairly trivial limitation of my program which limits the values of γ for a solution. The program cannot handle quarters with θ>180°, especially when we transform the first set of parameter in the second one thanks to the function '`getparam`'. This is a purely computational limitation, and it does not mean that cell with such quarters would not exist. Another version of '`getparam`' which would handle the case of quarters with θ>180° would be sufficient but is not necessary for getting interesting results. Indeed, the cells with such quarters are never optimal compared to other shapes with more edges.

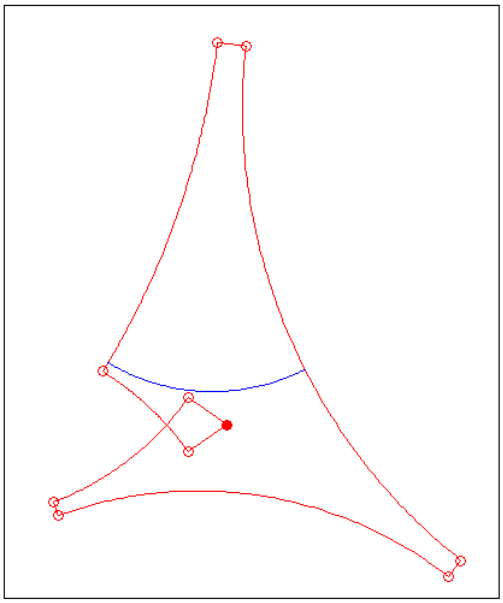

Figure 18. 7-edged solution of Type 2, with γ=-70°.

The gamma-plane is "bigger" than a normal 2D-plane. Notice the three edges which will trigger the geometrical limitation.

4. Results – Discussion

4.I. Topological results

4.I.a Details about Existence Domains

As mentioned in 'Abstract', we have computed the limits of the existence domain from the deterministic Errera's rule point of view. These limits are computed thanks to our program of cell division. They correspond to the parameter γ from which the dividing plane which led to the self-similar daughter is no longer optimal. Below is an example of visual results of this study. This enables to tell us boundaries out of which the shape could not really been observed.

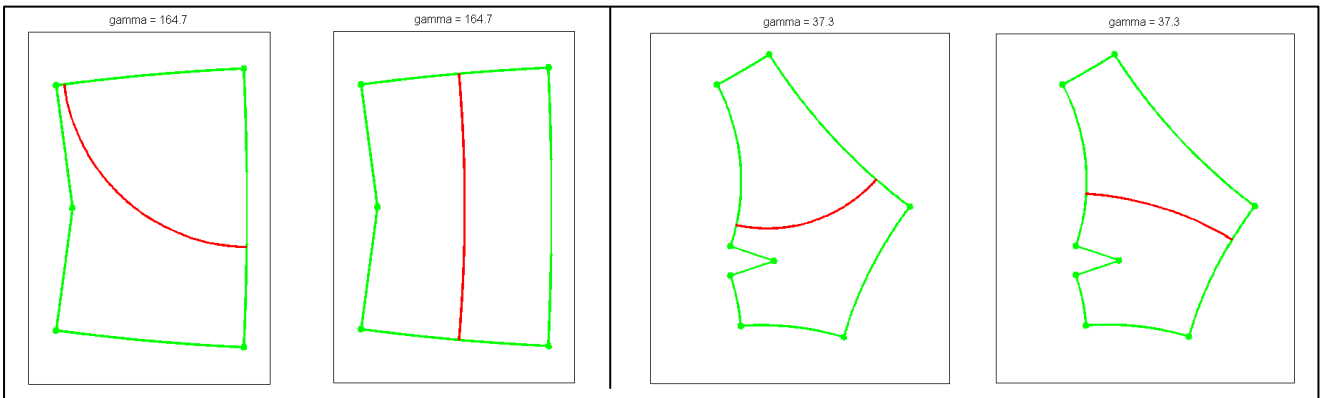

Figure 19. Visual examples of Existence domain boundaries

On the left is the "bottom" boundary for n=2: if γ <164.72°, the optimal dividing wall will lead to a 3-edged cell. On the right is the "top" boundary for n=5: if γ>37.2°, the optimal dividing wall lead to a cell with n'=n-1=4.

4.I.b Transitions

Nevertheless, we could go one step further to discriminate between the different shapes in regard to the parameter γ. Indeed, we can assume that the entire dynamic system will perform a global optimization, more than only the dividing cell. From that point, the system will quickly converge to the shape which will minimize the length of the new dividing wall for a given area of the cell, for every value of γ. In REF, we present the perimeter of this new wall in relation to the angle γ of the cone, which enables us to discriminate between different regimes of shapes. The numerical values for these transitions are summed up in REF.

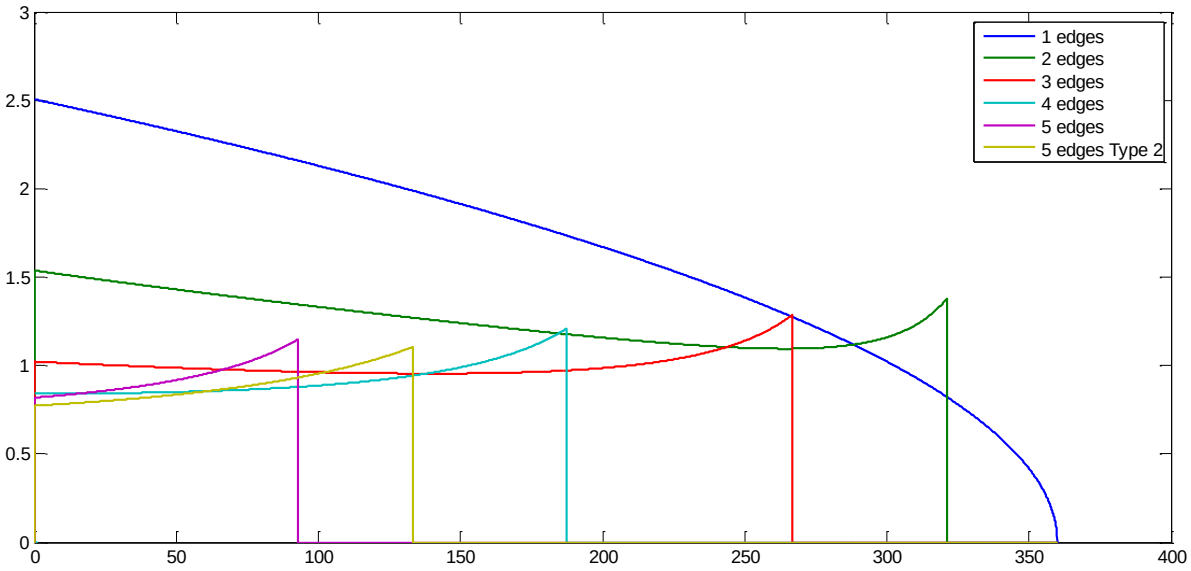

Figure 20. Length of the dividing wall in relation to the angle γ for different cell shapes with a normalized area

Figure 21. Summary of the different regimes for the cell shapes.

The transition angle between n=4 and n=5T2 is equal to 61.2°, but the top boundary of the shape for n=5T2 is lower, equal to 25.5°. Nevertheless, there is no room for n=5T1 since the last transition angle, between n=4 and n=5T1 is even smaller, equal to 16.3°.

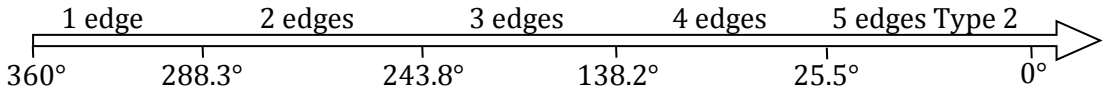

4.II. Validity of simulation

4.II.a Static versus Dynamic

Of course, the validity of this research is not wholesome. It doesn't provide us with a complete screening of the equilibrium landscape – in many dimensions – of our problem, even with the strict constraints we have set. Indeed, we have only looked for fixed points, but we have not (yet!) carried out dynamic simulations of cells dividing on the cone, and we don't know how stable are these shapes. Nevertheless, our static approach is really relevant, since it gives us a good criteria for topological sorting, and provide us with examples that are surely asymptotic points of the system.

I did not have the time to test for the stability of these fixed point solutions, but it should be the first dynamic test carried out, and all the tools are at hand (crafted during this project!). Then, it will be really interesting to start from a random shape and to see how fast it converges to which shape (or sequence of shapes).

4.II.b One trial of application

To show the qualitative relevance of our research, I will try to "fit" solutions to a real sample, and see how they match. This task is carried out throughout the following figure.

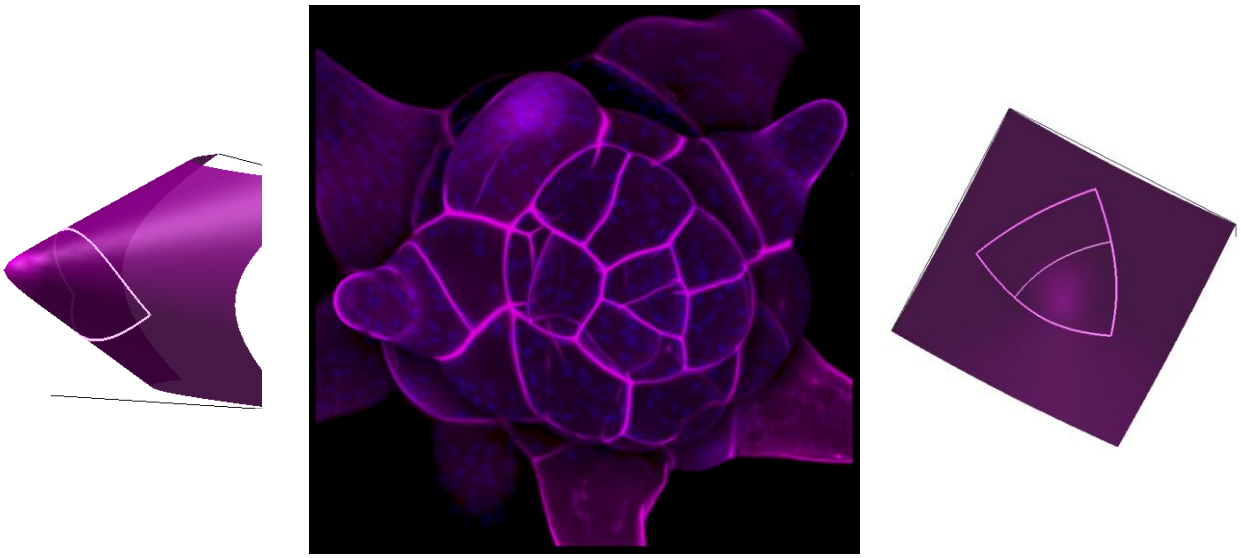

Figure 22. SCM shot of a gnagna foam.

ANNEXES

Annex 1: help sections of programs.

1. 'histv2'

```
%HIST V2 "Window" Histogram
%This function takes the syntax from the built in function "hist", but
%enables to have a "sliding window" count instead of a simple histogram.
%Indeed, you can specify, after the first integer which denotes the window
%width, a second integer which let you fix a number of points you want to
%be plotted.

%For instance, histv3(Y,a,b) will give you b bins, but of a width equal to
%the bins which would have been considered with the command hist(Y,a).

%This function does not support all the features of the built in hist
%function. In particular :
% - you cannot specify a vector for the bins
% - the easy plot abilities are not implemented (but you should prefer the
% classic "plot" function instead of the "bar" function which is used by
%the built-in "hist" function for easy plot).

%Remark : Because of the renormalization undergone for points whose
%window goes beyond the range of the data sample, the sum of the points (in
"no"), even
%if divided by the ratio b/a, will not exactly be equal to the initial
%amount of point initially present in the Y vector.

%See also : hist, hist2, Test_histv2

%   Copyright 2011 Antoine Lizée
%   $Revision: 1.0 $Date: 2011/05/18$
```

2. 'hist2'

```
%%HIST2 "Softened" Histogram

%SUMMARY:
%This function takes all the abilities of the built-in "hist" function,
%but it computes the numbers of points for bins that are different
%(somehow wider)than the original bins. It enables the user to compute an
%histogram that get rid of the fast variations. See MEANING for further
%explanation.

%SYNTAX :
%- N=hist2(Y,M) is the same as hist2(Y,M,1)
%- N=hist2(Y,M,z), Y is a vector of points or an array. M is the number of
%initial bins, and z is the level of "softening". z is also the number of
%neighbor bins taken into account to calculate the value for each initial
%bin (see PRECISIONS).
%- N=hist2(Y,X,...), X is a vector specifying bin centers (see "hist").
%Although this function is supported, you are not advised to use it.
%- [N X]=hist2(...) is a supported syntax (see "hist")
%- hist2(...) is a supported syntax (see "hist")

%PRECISIONS
%The value n computed for each bin is the result of a weighting of the
%neighbor bins depending on the third arg "z" as follows :
```

```
%
%
%
% z                                  plotted bin     3rd right neighbor
%|||                                    |||               |||
% 0     0     0     0     0     0     1     0     0     0     0     0
% 1(def)0     0     0     0     1     1     1     0     0     0     0
% 2     0     0     0     1     2     3     2     1     0     0     0
% 3     0     0     1     3     6     7     6     3     1     0     0
% 4     0     1     4    10    16    19    16    10     4     1     0
% 5     1     5    15    30    45    51    45    30    15     5     1
% etc...
% It is then normalized by the sum of the coefficients used for each bin,
%in order to unchange the total number of points. The computation of the
%extremities of the sample are slightly different.

%THESE coefficients, for z>1, are a very close approximation of a
%normalized gaussian,centered at 0 and of standard deviation equal to :
% sigma=sqrt(2/3*z).

% MEANING :
%For the first step (z=1), hist2 is a M-point histogram with
%(range(Y)/M*3)-wide bins (three times larger than the initial ones).
% (See "histv2")
%For any further step, the weigthing carried out by hist2 can have the two
%following precise meanings :
% - from a probability point of view, it computes the distribution of the
%law resulting from the sum of the initial law corresponding to the classic
%histogram and a normal law, centered in zero and of std sigma. This
%represents a quantification of the error due to discretisation of the
%probability distribution.
% - from an analytic point of view, it computes the convolution of the
% distribution function of the sample with a gaussian function, centered
%in zero and of standard deviation sigma. As a result, we got  the
%distribution function in which we have gradually and smoothly erased all
%variations which have a half-period smaller than the typical half period :
% T/2=pi*STD=pi*sigma.
%We put here these values versus some z values :

%     z         | 2 | 3 | 4 | 5 | 6 | 7 | 8 | 9 | 10| 15| 22 | 30 | 39 | 61 | 95
%-------------------------------------------------------------------------------
%typical half-  |3.6|4.4|5.1|5.7|6.3|6.8|7.3|7.7|8.1|9.9|12.0|14.0|16.0|20.0|25.0
%period of rejection (in bins)

% SEE ALSO : hist, histv2, Test_hist2v2

%   Copyright 2011 Antoine Lizée
%   $Revision: 1.0 $Date: 2011/05/10$
```

Annex 2: Analysis of « plotedges.mat »

Comparison of the characteristics pointed out by the plotedges function

1. Introduction

These representations of the different tissues arise from a simple method of tissue analysis. We consider all the vertices of the selected numerical tissue and we sort all of them depending on characteristics of the three edges of each vertex. The first step is to choose one principal edge for each vertex, and then we rotate the vertex in order to put this edge on the Xaxis, on the right. The second – facultative – step is then to flip the vertex, if needed, to perform another sorting between the two remaining edges, on the bottom and the top of the graph.

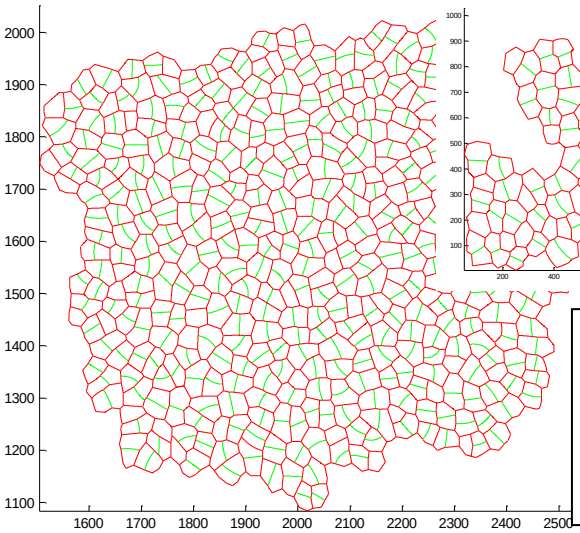

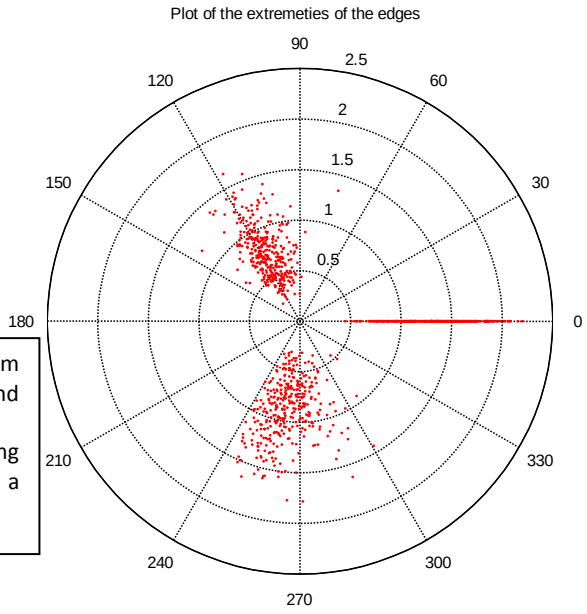

Numerical tissues from images of Zinnia (left) and Microsorum (top).
On the right, the plotting of 410 vertices from a Microsorum tissue.

1.I. Choices

Here, we choose to sort the edges depending on the angles, because we assume that it is the most reliable criterion to characterize the geometry of the tissue, especially as the youngest edges (new wall cells) are very well represented by being in front of the largest angle. We will compare this approach to a sort by size later.

- First choice: we put on the right the edge which is assumed to be the youngest, in front of the biggest angle. Therefore the largest angle is on the left.
- Flipping of the vertices: we enable the flipping of the vertices, in order to put the bigger of the two remaining angles on the top of the graph.

1.II. Remarks

⇒ The extremity of the edges plotted is an “extended” extremity in the sense that we unroll the possible bend of the edge, and we keep the angle at the vertex.

⇒ The tissues that we will compare to test this representation are 5 tissues from leafs of the same system, of the species “Microsorum”; and one tissue, four times larger, of the meristem of a system from the species “Zinnia”.

⇒ Some treatment can be carried out after the sorting. In all the representations of this document, we have normalized the length of the edges by the mean of the length of the three edges for each vertex.

⇒ The difference between 'low' sorting (only with the first step) and full sorting is remarkable in a tissue such as Microsorum. Here we show the representations for the 4th tissue of Microsorum in 'low' mode. You can compare the data analysis (left) with the following graphics to be followed (next page) and the plot with the first one (previous page, same sample). The flipping of the vertices, logically enough, lead to an asymmetry between the repartitions in angle and size.

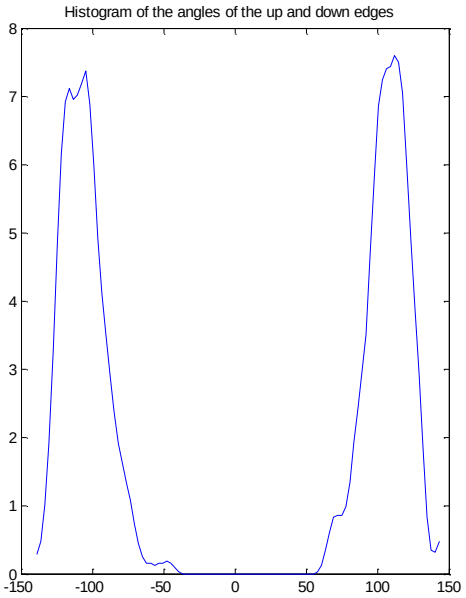

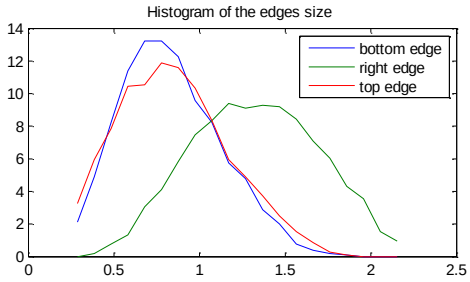

Concerning the angles :

	bottom angle	left angle	top angle
means :	106.0	147.2	106.8
std dev. :	15.4	17.0	14.5

Concerning the sizes :

	bottom edge	right edge	top edge
means :	0.83	1.32	0.85
std dev. :	0.28	0.36	0.31

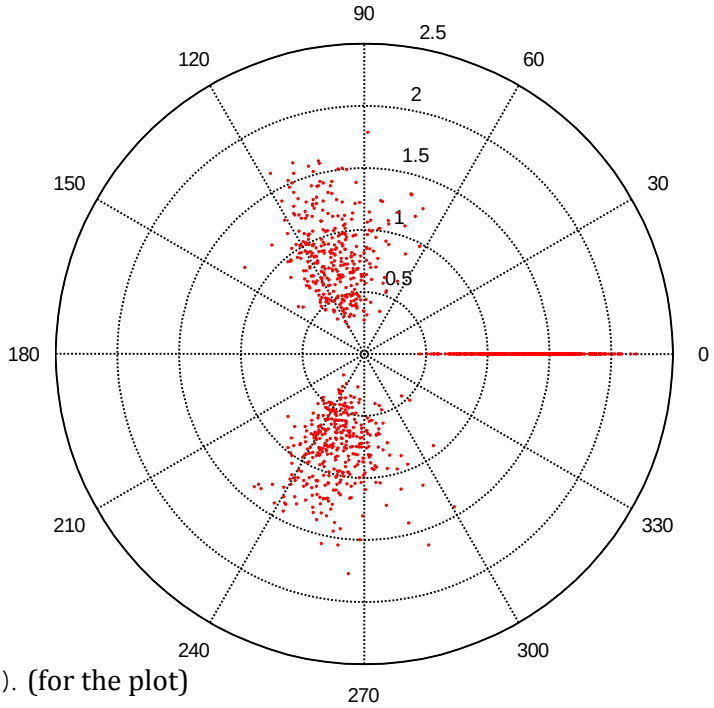

For information, such graphs
are the result of these two lines of code:

-> plotedges(originaltissue,'normmean','low'). (for the plot)

-> plotedges(originaltissue,'normmean','hist','stat','sub','no','histsize','low') (for the data anylisis)

2. Data analysis

Here we present summaries of the data analysis of the distribution of the edges extremities for each tissue

Microsorum 1

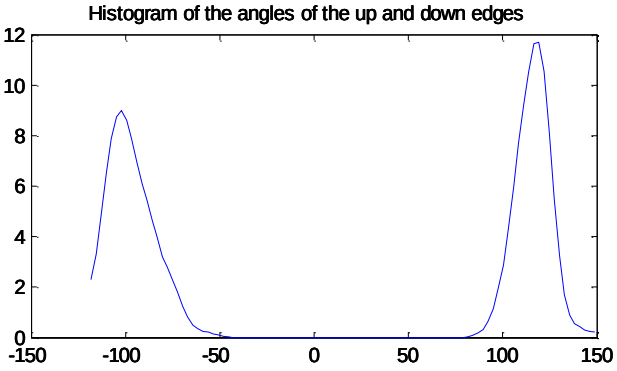

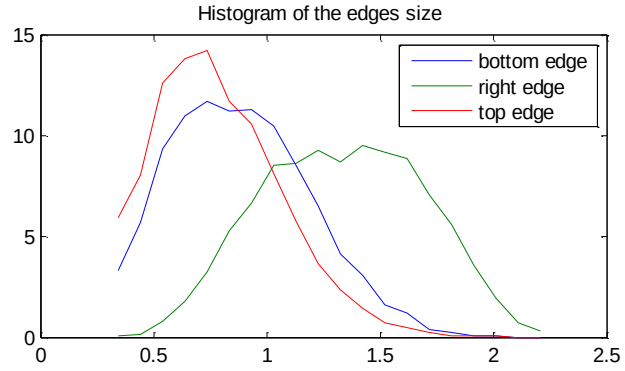

Concerning the angles :			
	bottom angle	left angle	top angle
means :	96.7	147.3	116.0
std dev. :	12.4	15.5	9.2

Concerning the sizes :			
	bottom edge	right edge	top edge
means :	0.88	1.33	0.78
std dev. :	0.30	0.35	0.27

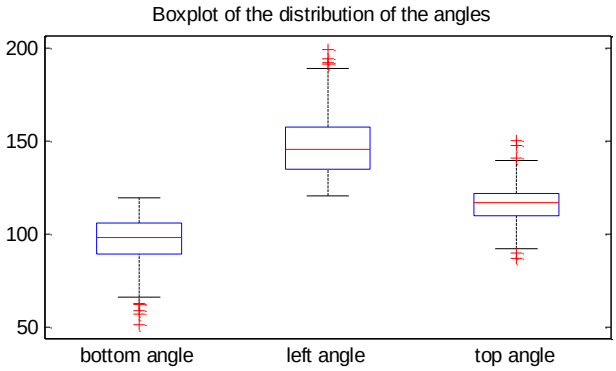

Microsorum 2

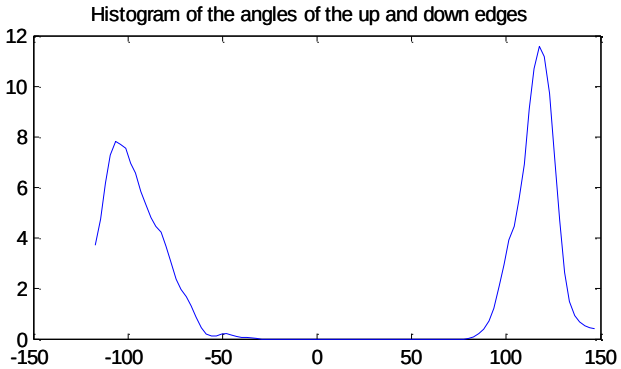

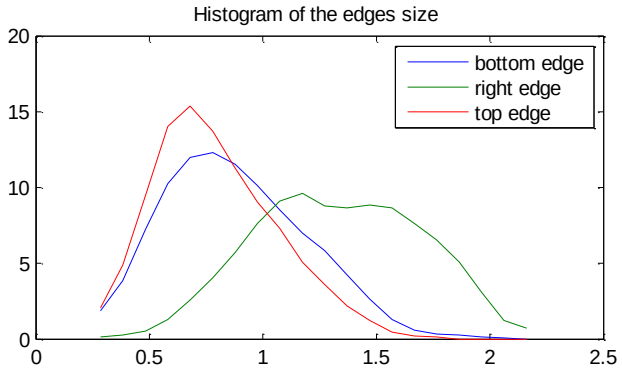

Concerning the angles :			
	bottom angle	left angle	top angle
means :	95.8	148.3	115.9
std dev. :	14.1	17.3	9.8

Concerning the sizes :			
	bottom edge	right edge	top edge
means :	0.88	1.33	0.79
std dev. :	0.30	0.36	0.26

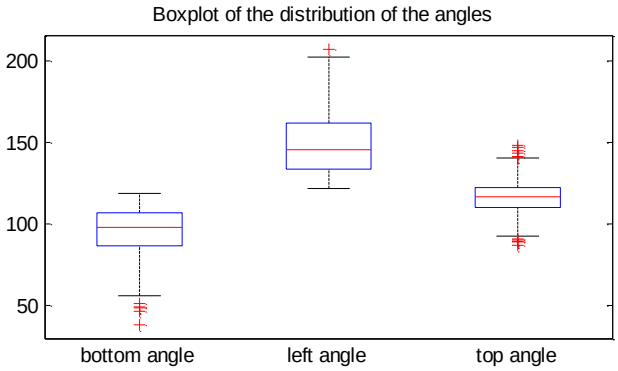

Microsorum 3

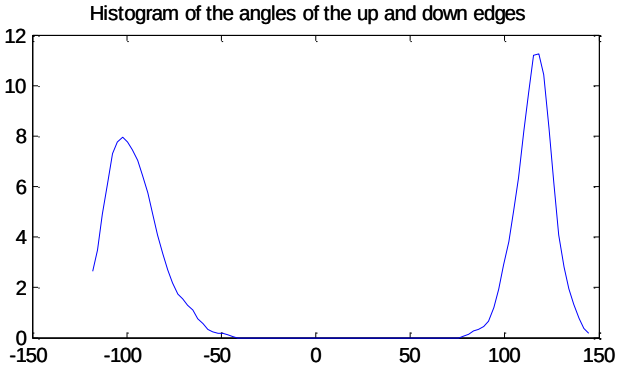

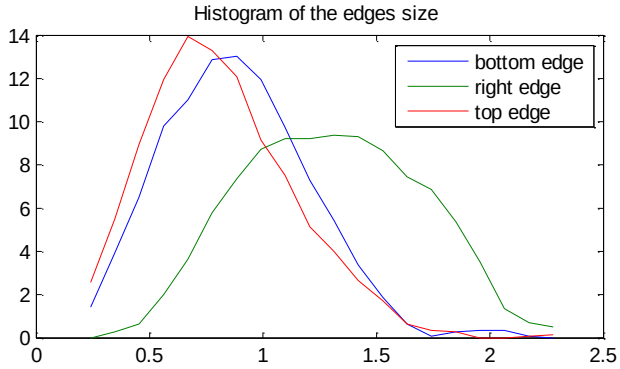

Concerning the angles :

	bottom angle	left angle	top angle
means :	95.8	148.5	115.7
std dev. :	13.5	16.8	9.8

Concerning the sizes :

	bottom edge	right edge	top edge
means :	0.88	1.30	0.82
std dev. :	0.31	0.38	0.31

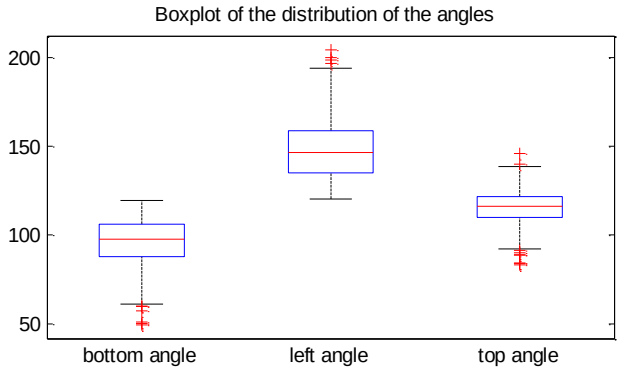

Microsorum 4

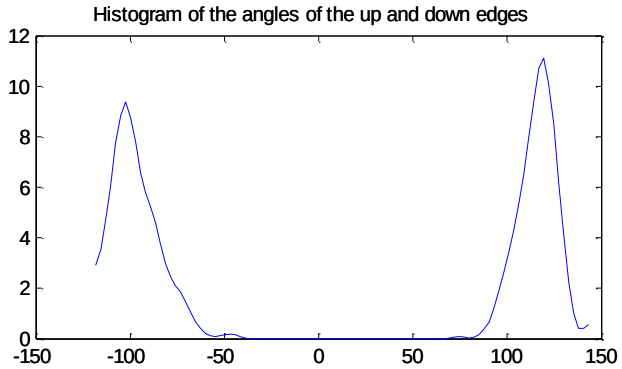

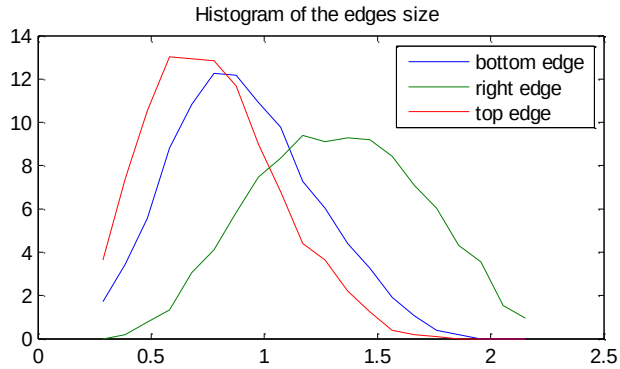

Concerning the angles :

	bottom angle	left angle	top angle
means :	97.0	147.2	115.8
std dev. :	13.0	17.0	10.1

Concerning the sizes :

	bottom edge	right edge	top edge
means :	0.91	1.32	0.77
std dev. :	0.30	0.36	0.27

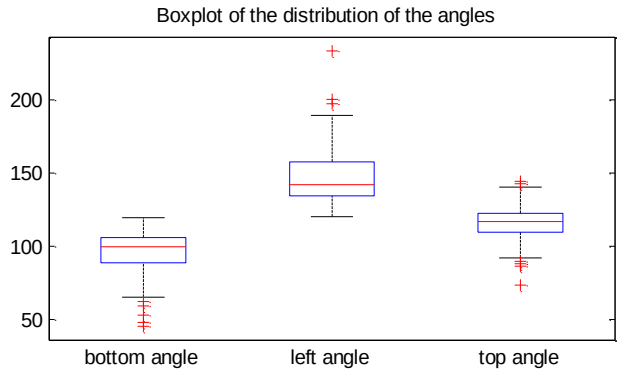

Microsorum 5

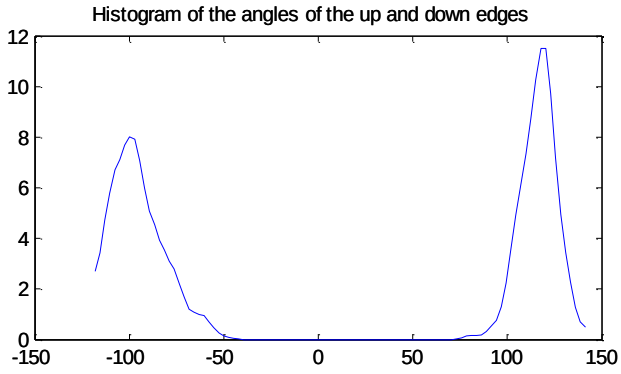

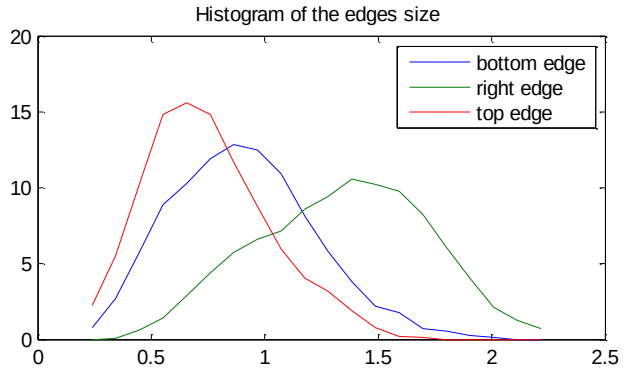

Concerning the angles :

	bottom angle	left angle	top angle
means :	95.2	148.4	116.4
std dev. :	14.0	16.4	9.5

Concerning the sizes :

	bottom edge	right edge	top edge
means :	0.91	1.34	0.75
std dev. :	0.31	0.36	0.26

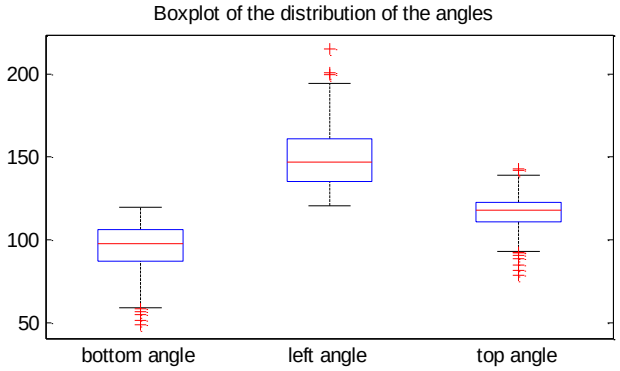

Zinnia

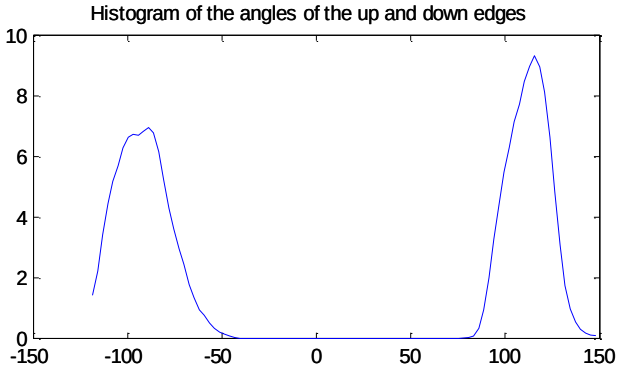

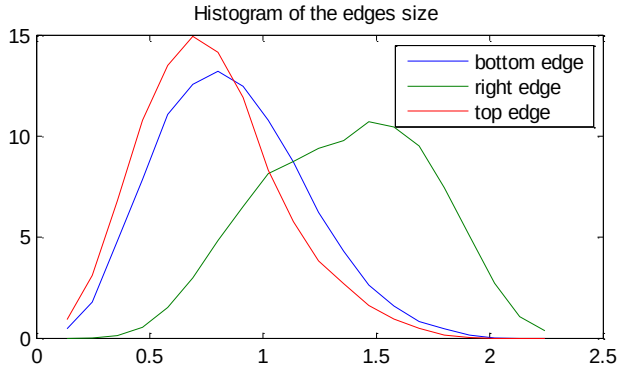

Concerning the angles :

	bottom angle	left angle	top angle
means :	91.9	155.8	112.3
std dev. :	13.8	17.6	10.4

Concerning the sizes :

	bottom edge	right edge	top edge
means :	0.86	1.36	0.77
std dev. :	0.31	0.36	0.29

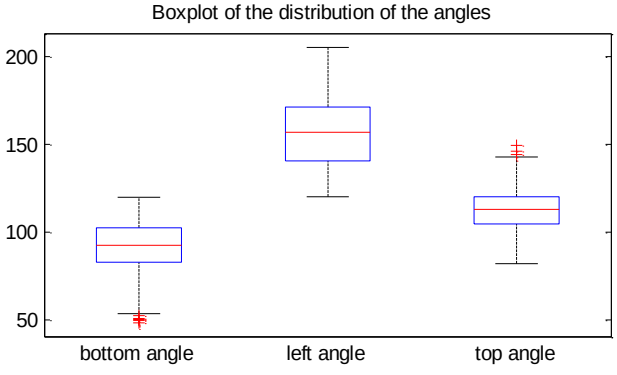

2.I. Comments

We can witness the homogeneity of the five tissues from Microsorum. It implicates that such a representation of the tissue is relevant. Moreover, the Zinnia tissue which seems really close to the Microsorum tissues visually, have data summary which proves out to be similar in many ways, excepted the difference between the means of the angle and the edges length. The bigger left angle and the taller right edge imply that the tissue is “overally” younger, or more active concerning divisions. Here are the two histograms with Zinnia (bold then solid line) and the five Microsorum :

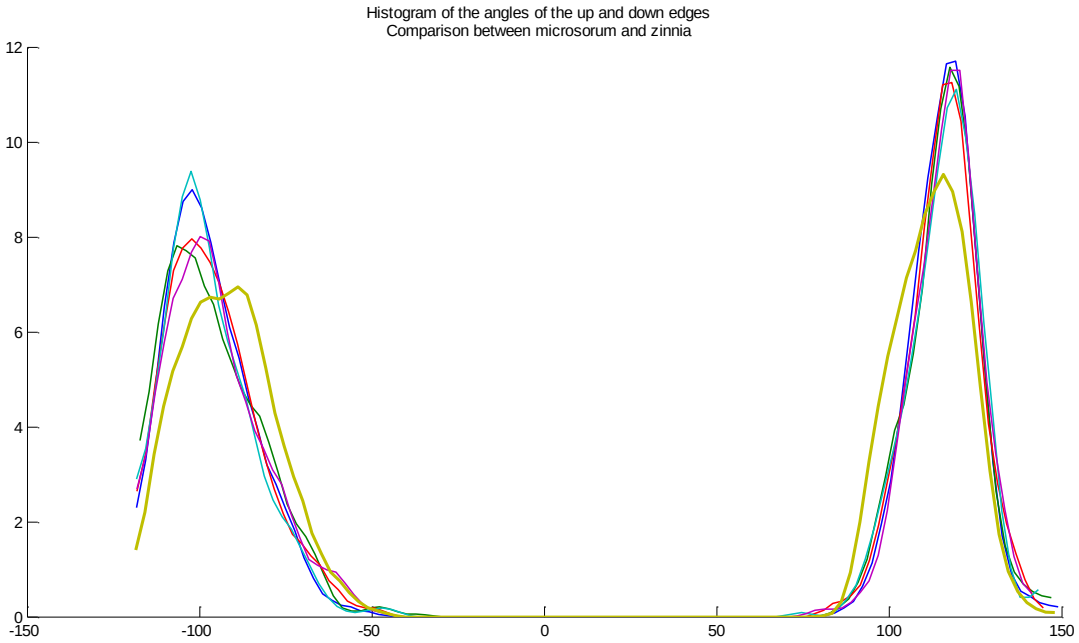

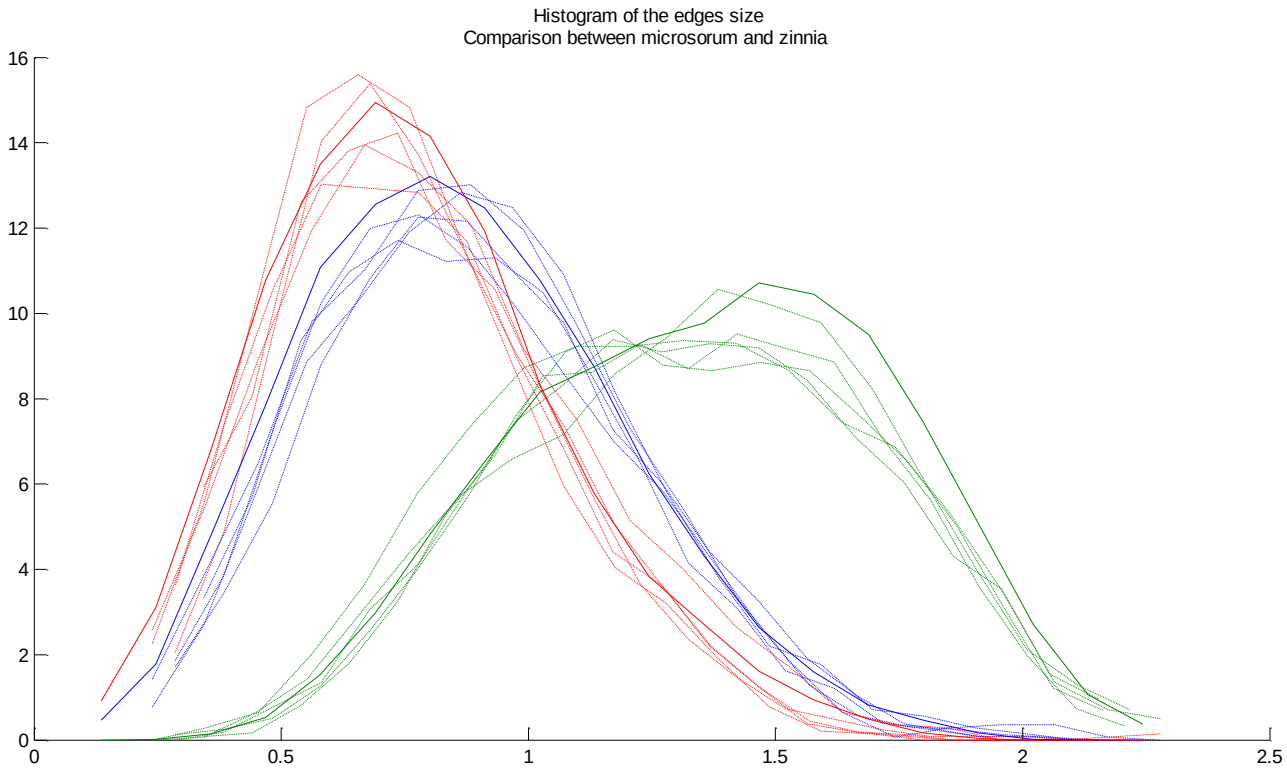

3. Hillocks representation

Here we represent a “virtual view” which we obtain by piling little hillocks at each location we would have plotted an edge extremity. Each “hillock” is a Gaussian of a chosen variance w. Thus, we obtain a sort of 3d histogram, which can be represented on a 3d view (see first figure) but also in plots with level lines, which we prefer for comparison.

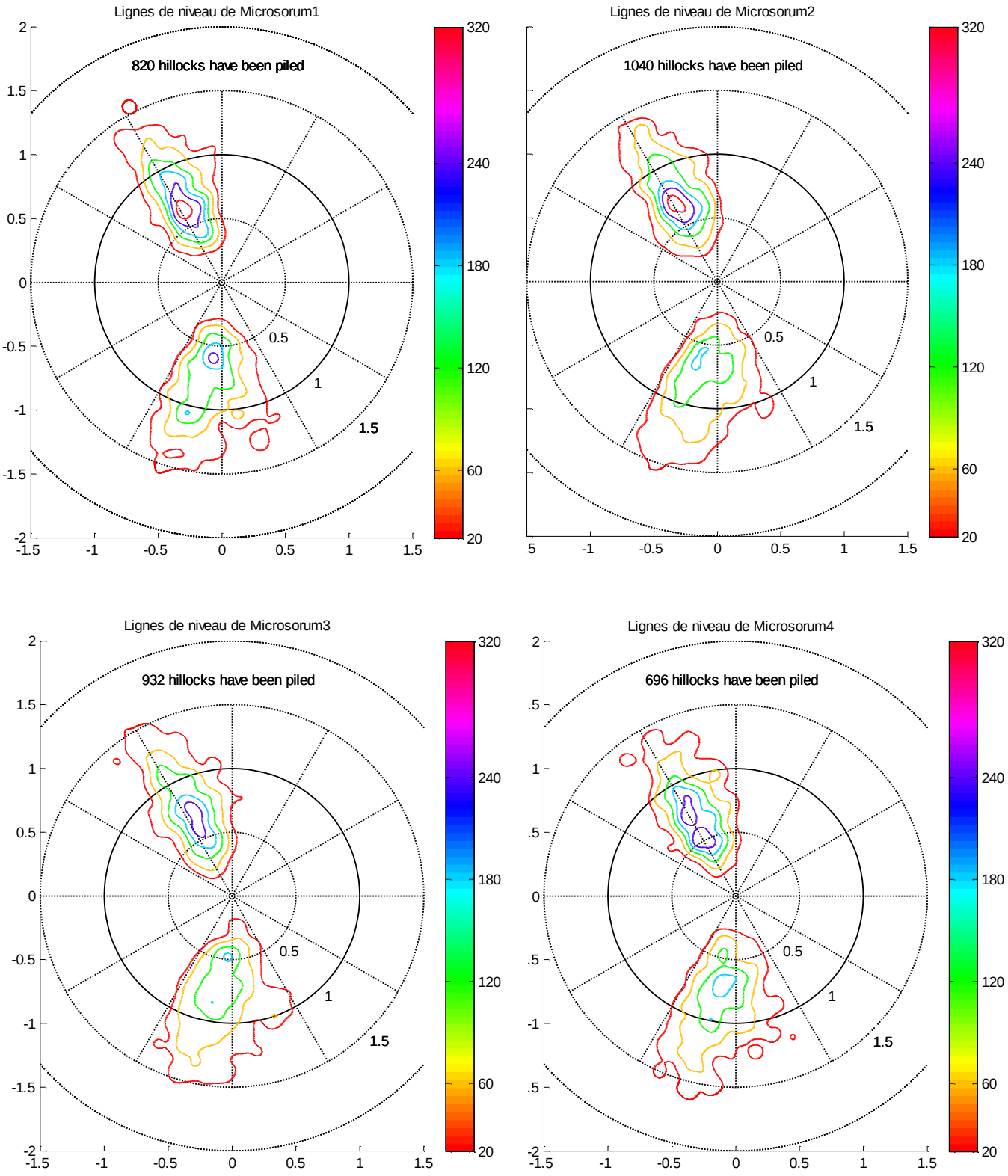

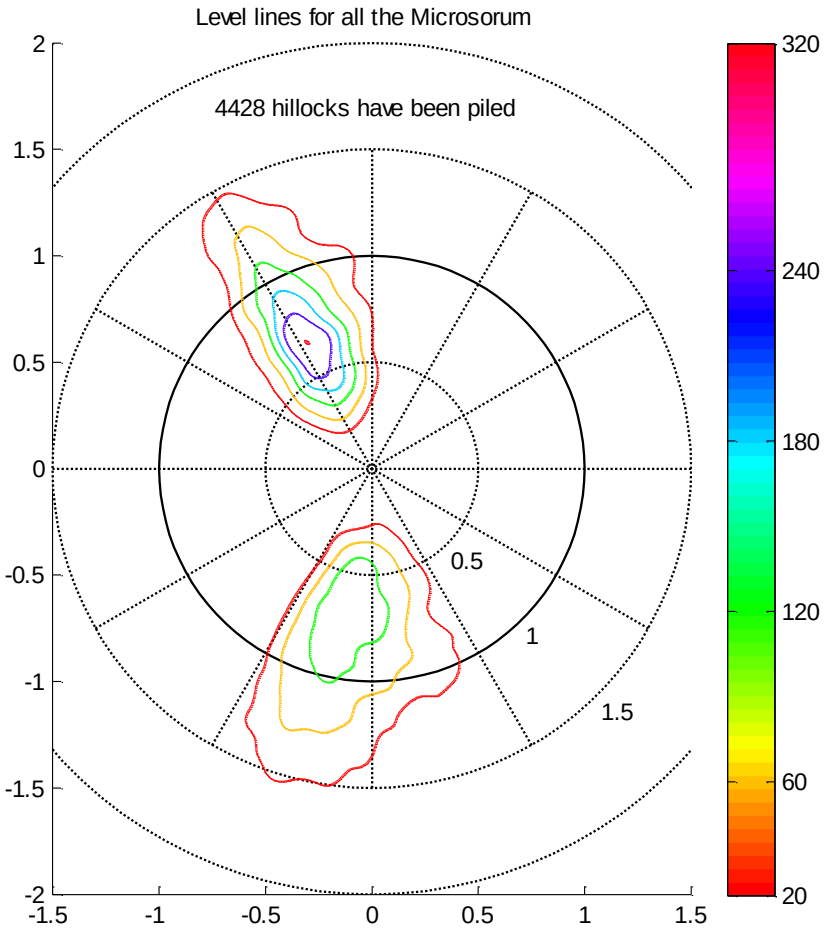

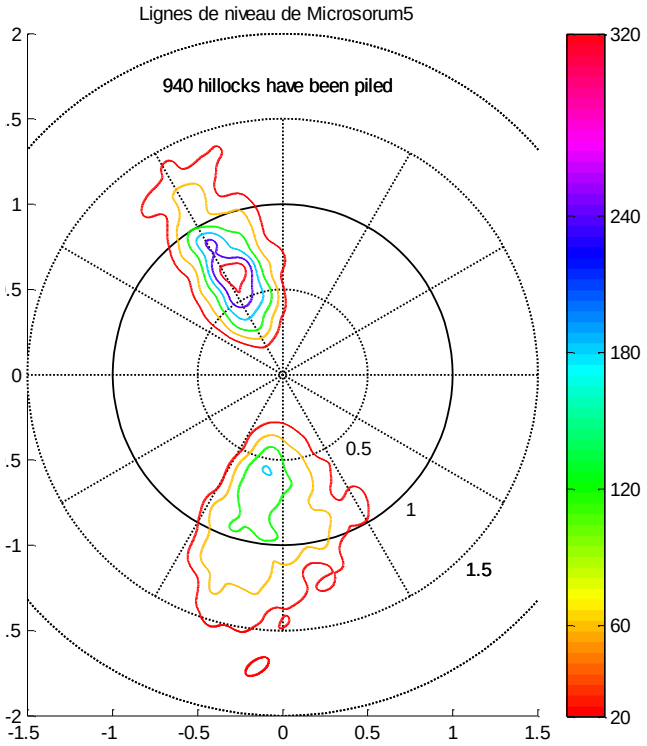

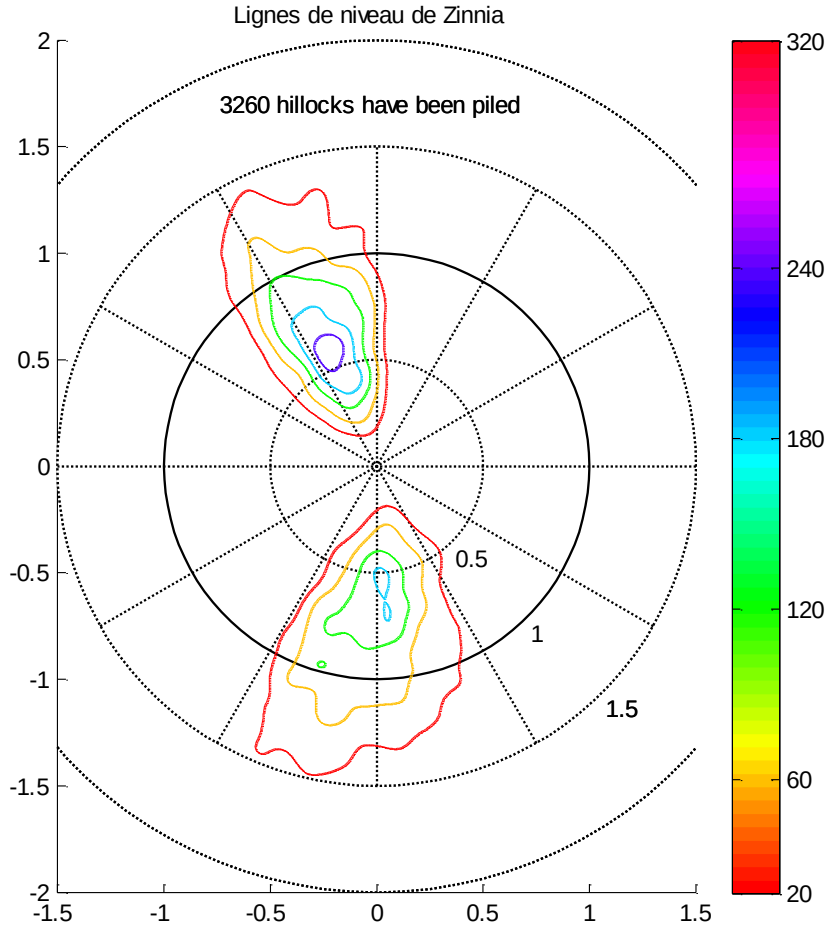

This provide us with a more visual representation of this analysis of sample tissues. We can draw the two same conclusions from these representation and the previous exposition of data :

- All the tissues have the same property and overall values, which corroborate the fact that these tissues are visually very similar. Nevertheless, each sample has its own representation. This method of tissue analysis seems therefore relevant.
- This study enable us to make out a difference between the two pattern that we could not see without such a tool. These differences emanate from a same real characteristic : the activity of the tissue in term of division. Zinnia, with more asymetric distributions (right edge longer and left angle bigger), is a “younger” tissue, denoting a more intense division activity or a slower relaxation behaviour.